Spin-lattice relaxation in an isotropic elastic continuum with spherical lattice waves and a cubic crystal field*

E. R. Bernstein and D. R. Franceschetti†
Department of Chemistry, Princeton University, Princeton, New Jersey 08540
(Received 29 October 1973)

Spin-lattice relaxation among hyperfine levels of the cubic systems $CaF_2:Tm^{2+}$, $CaF_2:Ho^{2+}$, and $MgO:Er^{3+}$ is studied theoretically from zero to high magnetic fields. Relaxation-rate expressions are derived employing a description of lattice dynamics in terms of normal modes of vibration transforming as spherical harmonics. Full use is made of symmetry considerations in formulating the ion-lattice interaction Hamiltonian and the computation of transition rates. Relaxation between ion levels not derived from a time-conjugate pair of electronic states is discussed in detail, with particular attention to the Raman process which may exhibit a complex temperature dependence in such cases. Relaxation rates are calculated from a crystal-field model and isotropic-elastic-continuum lattice dynamics. The systems $CaF_2:Tm^{2+}$ and $CaF_2:Ho^{2+}$ exhibit a small direct process, a T^9 Raman process, and an $e^{-\Delta/kT}$ resonance Raman process ($CaF_2:Ho^{2+}$ only). $MgO:Er^{3+}$ exhibits a large direct process, a complex Raman process with temperature dependence a sum of terms $T^n (n = 5,...,9)$, and the usual $e^{-\Delta/kT}$ resonance Raman process. Calculated results are found to be quite sensitive to the value of $\langle r^2 \rangle$ employed. Reasonable agreement with the available experimental data is obtained.

I. INTRODUCTION

Relaxation of paramagnetic ions in diamagnetic crystal hosts has been extensively studied by many authors.[1] While qualitative features appear to be understood, quantitative agreement of theory with experiment awaits a deeper understanding of ion-ligand interactions and dynamics of ionic crystal lattices. Theoretical approaches in this area might conveniently be divided into three broad categories. The phenomenological approach of Orbach[2] and Scott and Jeffries,[3] in which static crystal-field parameters are employed in approximating ion-lattice interactions and contributions of all lattice vibrational modes are approximated in a single effective-strain operator, has been reasonably successful, particularly in describing relaxation of rare-earth ions in low-symmetry environments. In contrast, Van Vleck[4] and others[5,6] have chosen to work within a well-defined simple model in which *ligands are described as point charges* and *lattice dynamics simulated by isotropic-elastic-continuum mechanics*. Aside from a physically motivated assumption that relaxation involves primarily long-wavelength vibrational modes, relaxation rates calculated within this model system are obtained without mathematical approximation. More recently, Stedman and Newman[7] employed a detailed model, in which experimentally determined interionic force constants were employed together with a more sophisticated model of dynamic ion-ligand interactions.

The study of spin-lattice relaxation detailed in this paper falls clearly into the second (well-defined model system) category. Our primary objective is to place the results for a simple but effective model into a form in which the physics of the relaxation process is most obvious. We feel that results cast in this form will be of greater heuristic value for more detailed calculations and will also serve as a reasonable description of the phenomenon itself.

A particularly simple physical picture for relaxation processes can be formulated in terms of a description of the lattice dynamics based on "spherical waves," i.e., normal modes transforming as spherical harmonics. Such an approach is especially well suited to the point-source nature of relaxing ions in a nonmagnetic host lattice.[8] It will be shown that in a spherical wave formulation, to an excellent approximation, only a few lattice normal modes are coupled to the paramagnetic ion, in contrast to conventional plane-wave formulations, in which all lattice modes are involved. Further, the spherical-wave approach eliminates the tedious process of "averaging over all directions of polarization and propagation,"[4,5] while providing rigorous and equivalent results. Development of this approach was motivated by our previous observation[9] that the phenomenological Hamiltonian of Orbach[2] and Scott and Jeffries[3] is a scalar product of spherical tensor operators acting on electron and lattice coordinates.

Recently, several authors[5,10,11] have stressed the use of symmetry considerations to simplify spin-lattice relaxation calculations, particularly in minimizing the number of independent "dynamic crystal-field parameters." In the present study of spin-lattice relaxation among hyperfine levels at cubic sites, a group-theoretical approach is carried out to its logical conclusion, employing lattice-vibrational modes transforming as irreducible

representations of the paramagnetic-ion-site symmetry group. Cubic-lattice modes are constructed from a basic set of spherical modes in a manner analogous to construction of ion crystal-field states from a set of angular momentum eigenstates. Use of such normal modes simplifies calculation of matrix elements of the orbit-lattice interaction and provides a clearer physical picture of spin-lattice relaxation processes. The group-theoretical formulation would appear to be an essential preliminary to more sophisticated calculations, particularly in treating such systems as S-state ions, for which the most reliable knowledge of ion states is group theoretical in form.

Calculated spin-lattice relaxation rates for hyperfine levels of the systems $CaF_2:Tm^{2+}$, $CaF_2:Ho^{2+}$, and $MgO:Er^{3+}$ from zero to very high magnetic fields are presented. For clarity the presentation is broken up into sections, each dealing with one aspect of the calculation. Section II describes construction of a lattice Hamiltonian in terms of spherical waves and in terms of linear combinations of spherical waves transforming as rows of irreducible representations of the cubic (O_h) group. In Sec. III the most general ion-lattice interaction possible at a cubic site is discussed and general expressions for relaxation rates between ion states are derived using lattice-strain matrix elements evaluated in the cubic basis of Sec. II. In Sec. IV electronic and hyperfine states of the systems studied are given. Section V presents a novel rederivation of Buisson and Borg's[5] ion-lattice Hamiltonian in a crystal-field model. Section VI contains calculated relaxation rates and compares them with available experimental data. Attention is focussed on relaxation at zero external field, a topic of concurrent experimental study.[12] Finally, Sec. VII assesses utility and limitations of the method and indicates lines of future investigation.

II. LATTICE DYNAMICS: SPHERICAL WAVES

Assuming the lattice may be described as an isotropic elastic continuum (Debye model), the instantaneous configuration of the lattice is defined by a displacement vector field $\vec{s}(\vec{r}, t)$, which contains the displacement of each mass element from its equilibrium position $\vec{r}$. The potential energy density for an *elastic* continuum is a quadratic function of components of the strain tensor $\overleftrightarrow{\sigma} = \vec{\nabla}\vec{s}(\vec{r}, t)$. Components of $\overleftrightarrow{\sigma}$ can be written as elements of three irreducible tensorial sets[13]

$$\sigma_{nm} = \sum_q \nabla_q s_{m-q}(\vec{r}) \langle 1\, q\, 1\, m-q | 1\, 1\, n\, m\rangle , \qquad (2.1)$$

in which $n = 0, 1, 2$; $m = -n, \ldots, n$; and $\langle j_1 m_1 j_2 m_2 | j_1 j_2 j\, m\rangle$ is a Clebsch-Gordan coefficient. It is helpful to introduce cogredient sets of unit spherical dyadics

$$\overleftrightarrow{u}_{nm} = \sum_q \hat{e}_q \hat{e}_{m-q} \langle 1\, q\, 1\, m-q | 1\, 1\, n\, m\rangle , \qquad (2.2)$$

in which

$$\hat{e}_1 = -(1/\sqrt{2})\hat{e}_x - (i/\sqrt{2})\hat{e}_y , \qquad (2.3a)$$

$$\hat{e}_0 = \hat{e}_z , \qquad (2.3b)$$

$$\hat{e}_{-1} = (1/\sqrt{2})\hat{e}_x - (i/\sqrt{2})\hat{e}_y , \qquad (2.3c)$$

and $\hat{e}_x, \hat{e}_y, \hat{e}_z$ are unit vectors in the x, y, z directions. The strain dyadic (or second-rank tensor) then is expressible as

$$\overleftrightarrow{\sigma} = \sum_{n=0}^{2} \sum_{m=-n}^{n} (-1)^{n+m} \sigma_{nm} \overleftrightarrow{u}_{n-m} . \qquad (2.4)$$

For an *isotropic* elastic medium the potential energy density is a linear combination of quadratic functions of strain components, invariant under all rotations, namely,

$$U_n = \sum_p (-1)^p \sigma_{np}\sigma_{n-p} \quad (n = 0, 1, 2) . \qquad (2.5)$$

Further, U_1 is associated with a rotation, not a strain, and will not contribute to the elastic potential energy.[14] Thus, only two independent elastic constants appear in the potential-energy density. For cubic rather than isotropic media, U_2 reduces to the sum of two terms, corresponding to the Γ_3 and Γ_5 representation of the group O; there are three independent cubic elastic constants.[15]

The Lagrangian density for an isotropic elastic medium is conventionally written in the form[16]

$$L = \tfrac{1}{2}\rho \dot{\vec{s}}^2 - \tfrac{1}{2}\overleftrightarrow{S} : \overleftrightarrow{T} , \qquad (2.6a)$$

$$\overleftrightarrow{S} = \tfrac{1}{2}(\vec{\nabla}\vec{s} + \vec{s}\vec{\nabla}) , \qquad (2.6b)$$

$$\overleftrightarrow{T} = \lambda | \overleftrightarrow{S} | \overleftrightarrow{1} + 2\mu \overleftrightarrow{S} . \qquad (2.6c)$$

In Eqs. (2.6), ρ is the crystal density; $\overleftrightarrow{S}$ is the symmetric part of $\overleftrightarrow{\sigma}$, called the pure strain dyadic; $\overleftrightarrow{T}$ is the stress dyadic; and λ and μ are elastic constants.

Applying the variational principle we obtain the Lagrange-Euler equation

$$\rho \frac{\partial^2 \vec{s}}{\partial t^2} = (\lambda + 2\mu)\,\mathrm{grad}\,(\mathrm{div}\,\vec{s}) - \mu\,\mathrm{curl}(\mathrm{curl}\,\vec{s}) , \qquad (2.7)$$

which, after separation of space and time variables

$$\vec{s}(\vec{r}, t) = \vec{s}(\vec{r})\, e^{i\omega t} , \qquad (2.8)$$

yields the equation

$$-\rho\omega^2 \vec{s}(\vec{r}) = (\lambda + 2\mu)\,\mathrm{grad}\,[\mathrm{div}\,\vec{s}(\vec{r})] - \mu\,\mathrm{curl}\,[\mathrm{curl}\,\vec{s}(\vec{r})] . \qquad (2.9)$$

Solutions of Eq. (2.9) are the normal modes of the system.

It is possible to form spherical waves by linear combination of plane-wave solutions of Eq. (2.9). Selecting boundary conditions which allow plane-

wave solutions of Eq. (2.9) (cubical boundary), one has a nonspherical system and encounters conceptual difficulties in the rigorous formation of spherical waves. A more direct approach obtains if uniform boundary conditions on the surface of a sphere of radius R are assumed. Dirichlet boundary condition $\vec{s}(R, \theta, \varphi) = \vec{0}$, originally used by Debye,[17] are therefore employed.

Solving Eq. (2.9) in spherical coordinates, yields one longitudinal and two transverse families of solutions

$$\vec{s}_{L\,nm} = \left(\frac{n}{2n+1}\right)^{1/2} j_{n-1}\left(\frac{\omega}{v_L} r\right) \vec{Y}_{n\,n-1\,m} + \left(\frac{n+1}{2n+1}\right)^{1/2} j_{n+1}\left(\frac{\omega}{v_L} r\right) \vec{Y}_{n\,n+1\,m}, \quad (2.10a)$$

$$\vec{s}_{M\,nm} = i j_n\left(\frac{\omega}{v_T} r\right) \vec{Y}_{nnm}, \quad (2.10b)$$

$$\vec{s}_{Nnm} = -\left(\frac{n+1}{2n+1}\right)^{1/2} j_{n-1}\left(\frac{\omega}{v_T} r\right) \vec{Y}_{n\,n-1\,m} + \left(\frac{n}{2n+1}\right)^{1/2} j_{n+1}\left(\frac{\omega}{v_T} r\right) \vec{Y}_{n\,n+1\,m}, \quad (2.10c)$$

in which j_n are spherical Bessel functions and $\vec{Y}_{nlm}$ are vector spherical harmonics[18]

$$\vec{Y}_{nlm} = \sum_p Y_{lp}\, \hat{e}_{m-p} \langle l p\, 1\, m-p \,|\, l\, 1\, n\, m \rangle, \quad (2.11)$$

and

$$v_L = [(\lambda + 2\mu)/\rho]^{1/2}, \quad v_T = (\mu/\rho)^{1/2}$$

are, respectively, longitudinal and transverse velocities of sound.

In Eqs. (2.10) $n = 1, 2, \ldots$ and $m = -n, \ldots, n$ are the angular momentum quantum numbers associated with elastic-wave motion. For the longitudinal branch only, $n = 0$ is also allowed and the $\vec{s}_{L00}$ solution has a particularly simple form

$$\vec{s}_{L00} = j_1[(\omega/v_L)r]\, \vec{Y}_{010} \quad (2.12)$$

and satisfies the boundary condition $\vec{s}(R) = \vec{0}$ for values of ω such that

$$j_1[(\omega^L_{0q}/v_L)R] = 0. \quad (2.13)$$

There is, thus, a set of longitudinal normal modes of zero angular momentum

$$\vec{s}_{L\,00q} = a^L_{0q} j_1[(\omega^L_{0q}/v_L)r]\, \vec{Y}_{010}. \quad (2.14)$$

The normalization constant a^L_{0q} is given by

$$a^L_{0q} = \{\tfrac{1}{2} R^3 j_2^2[(\omega^L_{0q}/v_L)R]\}^{-1/2}, \quad (2.15)$$

so that

$$\int_{4\pi} d\Omega \int_0^R r^2\, dr\, \vec{s}^{\,*}_{L\,00q} \cdot \vec{s}_{L\,00q} = 1. \quad (2.16)$$

The $\vec{s}_{Mnm}$ (for all n) satisfy the boundary condition for values of ω such that

$$j_n[(\omega^M_{nq}/v_T)R] = 0 \quad (2.17)$$

and a set of normal modes

$$\vec{s}_{Mnmq} = a^M_{nq}\, i j_n[(\omega^M_{nq}/v_T)r]\, \vec{Y}_{nnm}, \quad (2.18)$$

with normalization constants

$$a^M_{nq} = \{\tfrac{1}{2} R^3 j_{n+1}^2[(\omega^M_{nq}/v_T)R]\}^{-1/2} \quad (2.19)$$

is obtained. The index q distinguishes among the allowed lattice frequencies; n, m, and q together play a role analogous to that of the wave vector.

Unfortunately, for $n = 1, 2, \ldots$, the normal modes $\vec{s}_{Lnm}$ and $\vec{s}_{Nnm}$ are mixed by the boundary condition. It is then necessary to seek values of ω such that some linear combination of $\vec{s}_{Lnm}$ and $\vec{s}_{Nnm}$ satisfies the boundary condition. Setting the normal and transverse components of the displacement field at the boundary equal to zero, normal modes are derived of the form

$$\vec{s}_{1nmq} = a\vec{s}_{Lnm} + b\vec{s}_{Nnm} = a^1_{nq}\left\{\vec{Y}_{n\,n-1\,m}\left[n j_{n+1}\left(\frac{\omega^1_{nq}}{v_T} R\right) j_{n-1}\left(\frac{\omega^1_{nq}}{v_L} r\right) + (n+1) j_{n+1}\left(\frac{\omega^1_{nq}}{v_L} R\right) j_{n-1}\left(\frac{\omega^1_{nq}}{v_T} r\right)\right] + \vec{Y}_{n\,n+1\,m}\left[[n(n+1)]^{1/2} j_{n+1}\left(\frac{\omega^1_{nq}}{v_T} R\right) j_{n+1}\left(\frac{\omega^1_{nq}}{v_L} r\right) - [n(n+1)]^{1/2} j_{n+1}\left(\frac{\omega^1_{nq}}{v_L} R\right) j_{n+1}\left(\frac{\omega^1_{nq}}{v_T} r\right)\right]\right\}, \quad (2.20)$$

with normalization constant given by

$$a^1_{nq} = \left\{\tfrac{1}{2} R^3 (2n+1)\left[n j_n^2\left(\frac{\omega^1_{nq}}{v_L} R\right) j_{n+1}^2\left(\frac{\omega^1_{nq}}{v_T} R\right) + (n+1) j_n^2\left(\frac{\omega^1_{nq}}{v_T} R\right) j_{n+1}^2\left(\frac{\omega^1_{nq}}{v_L} R\right)\right]\right\}^{-1/2}. \quad (2.21)$$

The complete set of normalized solutions of (2.9) consists of the modes $\vec{s}_{L\,00q}$, $\vec{s}_{Mnmq}$, and $\vec{s}_{1nmq}$. While it might seem that one of the original three families of solutions has been lost, this is not the case. The large majority of the $\vec{s}_{1nmq}$, with small intensity near the boundary, are predominantly either transverse or longitudinal, with a small ad-

mixture of the other polarization.

It is now possible to construct lattice and orbit-lattice Hamiltonians in terms of creation and annihilation operations for normal modes $\vec{s}_{Xnmq}$. Therefore, we introduce the momentum density

$$p_i(\vec{r},t)=\frac{\partial L}{\partial \dot{s}_i(\vec{r},t)} \quad (i=x,y,z),$$

$$\vec{p}=\rho\dot{\vec{s}}\ ; \tag{2.22}$$

form the Hamiltonian density

$$\mathcal{H}=\vec{p}^{\,2}/2\rho+\tfrac{1}{2}\overleftrightarrow{S}:\overleftrightarrow{T}\ ; \tag{2.23}$$

and make a normal-mode analysis

$$\vec{p}(\vec{r},t)=\sum_{Xnmq} p_{Xnmq}\vec{s}_{Xnmq}(\vec{r}), \tag{2.24a}$$

$$\vec{s}(\vec{r},t)=\sum_{Xnmq} s_{Xnmq}\vec{s}_{Xnmq}(\vec{r}). \tag{2.24b}$$

In computing the stress and strain dyadics, it is helpful to define dyadic spherical harmonics

$$\overleftrightarrow{Y}_{jlnm}=\sum_{p} Y_{lp}\overleftrightarrow{u}_{n\,m-p}\langle l\,p\,n\,m-p\,|\,l\,n\,j\,m\rangle\,, \tag{2.25}$$

with the convenient orthogonality property

$$\int_0^{2\pi}d\varphi\int_0^{\pi}\sin\theta\,d\theta\,\overleftrightarrow{Y}^{*}_{jlnm}(\theta\varphi):\overleftrightarrow{Y}_{j'l'n'm'}(\theta\varphi)$$
$$=\delta_{jj'}\delta_{ll'}\delta_{nn'}\delta_{mm'}\,.$$

The stresses and strains associated with the various normal modes can now be computed using

$$\vec{\nabla}j_l(kr)\vec{Y}_{jlm}=(l+1)^{1/2}kj_{l+1}(kr)\sum_{n=0}^{2}\overleftrightarrow{Y}_{j\,l+1\,n\,m}\begin{Bmatrix}1 & 1 & n\\ l+1 & j & l\end{Bmatrix}(-1)^{l+j+1}(2n+1)^{1/2}$$
$$+(l)^{1/2}kj_{l-1}(kr)\sum_{n=0}^{2}\overleftrightarrow{Y}_{j\,l-1\,n\,m}\begin{Bmatrix}1 & 1 & n\\ l-1 & j & l\end{Bmatrix}(-1)^{l+j+1}(2n+1)^{1/2}\,, \tag{2.26}$$

in which

$$\begin{Bmatrix}j_1 & j_2 & j_{12}\\ j_3 & J & j_{23}\end{Bmatrix}$$

has its usual meaning as a $6-j$ symbol.

Substituting normal-mode expansions (2.24) into the Hamiltonian density (2.23) and integrating over the volume of the sphere, the lattice Hamiltonian becomes

$$\mathcal{H}=\sum_{Xnmq}\frac{1}{2\rho}[p_{X\,n\,m\,q}p^{*}_{X\,n\,m\,q}+(\rho\omega^{X}_{nq})^2 s_{X\,n\,m\,q}s^{*}_{X\,n\,m\,q}]=\sum_{Xnmq}\frac{(-1)^m}{2\rho}[p_{X\,n\,m\,q}p_{X\,n\,-m\,q}+(\rho\omega^{X}_{nq})^2 s_{X\,n\,m\,q}s_{X\,n-m\,q}]\,. \tag{2.27}$$

This last form, in particular, reflects the spherical harmonic nature of the normal modes. It is of course necessary to exclude modes of angular frequency greater than a limiting frequency for each branch $\omega^{X}_{\mathrm{Debye}}$, so that the total number of vibrational modes is equal to $3N$, where N is the number of unit cells in the crystal. The Hamiltonian (2.27) is easily placed in second-quantized form, with annihilation and creation operators, respectively,

$$a_{Xnmq}=(2\hbar\omega^{X}_{nq}\rho)^{-1/2}[p_{Xnmq}-(-1)^m i\rho\omega^{X}_{nq}s_{X\,n\,-m\,q}], \tag{2.28}$$

$$a^{\dagger}_{Xnmq}=(2\hbar\omega^{X}_{nq}\rho)^{-1/2}[(-1)^m p_{X\,n\,-m\,q}+i\rho\omega^{X}_{nq}s_{Xnmq}],$$

$$\mathcal{H}=\sum_{Xnmq}\hbar\omega^{X}_{nq}(a^{\dagger}_{Xnmq}a_{Xnmq}+\tfrac{1}{2})\,. \tag{2.29}$$

Linear combinations of "spherical" normal modes of the same total angular momentum n, may now be constructed to transform as rows of the irreducible representations of the cubic group. The transformation coefficients $\langle l\,m\,|\,l\,\Gamma\,a\beta\rangle$, introduced in constructing scalar cubic harmonics

$$Y(l\,\Gamma a\beta)=\sum_{m}\langle l\,m\,|\,l\,\Gamma\,a\beta\rangle Y_{lm}\,, \tag{2.30}$$

are most simply employed. Thus $Y(l\,\Gamma a\beta)$ transforms as the βth row of the irreducible representation Γ and a (suppressed when not needed) distinguishes different combinations of the same Γ and β. It proves most convenient to use real transformation coefficients.[19] Cubic normal modes are constructed from spherical modes by the following linear transformation:

$$\vec{s}_{X\,n\,\Gamma a\beta\,q}=\sum_{m}\langle n\,m\,|\,n\,\Gamma a\beta\rangle\,\vec{s}_{Xnmq}\,. \tag{2.31}$$

Cubic normal coordinates can likewise be written

$$s_{X\,n\,\Gamma a\beta\,q}=\sum_{m}\langle n\,m\,|\,n\,\Gamma a\beta\rangle\,s_{Xnmq}\,, \tag{2.32}$$

so that the total displacement $\vec{s}(\vec{r},t)$ takes the "cubic" form

$$\vec{s}(\vec{r},t)=\sum_{X\,n\,\Gamma a\beta\,q}s_{X\,n\,\Gamma a\beta\,q}(t)\vec{s}_{X\,n\,\Gamma a\beta\,q}(\vec{r})\,. \tag{2.33}$$

To preserve, as far as possible, similarity between cubic and spherical harmonics, the notation

$$Y^*(l\,\Gamma a\beta) = c_{\Gamma\beta}\,Y(l\,\Gamma a\bar{\beta}), \tag{2.34}$$

analogous to

$$Y^*_{lm} = (-1)^m Y_{l\,-m}, \tag{2.35}$$

will be employed, thus defining the row $\bar{\beta}$ and the sign factor $c_{\Gamma\beta}$. Annihilation and creation operators for cubic modes then become, respectively,

$$a_{X\,n\,\Gamma a\beta\,q} = (2\hbar\omega^X_{nq}\rho)^{-1/2}(p_{X\,n\,\Gamma a\beta\,q} - ic_{\Gamma\beta}\rho\omega^X_{nq}s_{X\,n\,\Gamma a\bar{\beta}\,q}), \tag{2.36a}$$

$$a^\dagger_{X\,n\,\Gamma a\beta\,q} = (2\hbar\omega^X_{nq}\rho)^{-1/2}(c_{\Gamma\beta}p_{X\,n\,\Gamma a\bar{\beta}\,q} + i\rho\omega^X_{nq}s_{X\,n\,\Gamma a\beta\,q}), \tag{2.36b}$$

and the lattice Hamiltonian has the form

$$\mathcal{H}_{1\,\mathrm{att}} = \sum_{X\,n\,\Gamma a\beta\,q} \hbar\omega^X_{nq}(a^\dagger_{X\,n\,\Gamma a\beta\,q}a_{X\,n\,\Gamma a\beta\,q} + \tfrac{1}{2}). \tag{2.37}$$

A novel method for forming lattice modes transforming as rows of the irreducible representations of the cubic group from a set of plane waves is given in an appendix, as an instructive complement to the spherical-mode approach.

III. ION-LATTICE INTERACTION AND RELAXATION MECHANISMS

The Hamiltonian for the combined ion-lattice system is a sum of three terms

$$\mathcal{H} = \mathcal{H}_{\mathrm{ion}} + \mathcal{H}_{1\,\mathrm{att}} + \mathcal{H}_{11}, \tag{3.1}$$

in which the first two terms are the Hamiltonians for ion and lattice, respectively, while the third is the ion-lattice interaction. In systems discussed here the ion occupies a lattice site of O_h symmetry, assumed to be the origin of the coordinate system. In the absence of external fields, $\mathcal{H}$ will transform totally symmetrically in O_h. $\mathcal{H}_{11}$ can be expressed in terms of a series of products of lattice operators and ion operators. For the moment no assumptions as to the nature of the interaction are made, save that it is dependent on the relative coordinates of the ions embedded in the lattice.

Recall that the instantaneous configuration of the lattice is given, in a continuum model, by the displacement vector field $\vec{s}(\vec{r}, t)$. Thus, the paramagnetic ion, whose equilibrium position in the lattice is $\vec{R}^0_0 = \vec{0}$, will at time t be located at $\vec{R}^0_0 + \delta\vec{R}_0(t) = \vec{0} + \vec{s}(\vec{0}, t)$. Similarly, any other ion in the lattice, with equilibrium position $\vec{R}^0_i$, will at time t be located at $\vec{R}_i + \delta\vec{R}_i(t) = \vec{R}^0_i + \vec{s}(\vec{R}^0_i, t)$. The displacement $\delta\vec{R}_i$, is represented in a Taylor series as

$$\delta\vec{R}_i = \vec{s}(\vec{R}^0_i) = \vec{s}(\vec{0}) + \vec{R}^0_i\cdot\vec{\nabla}\vec{s}(\vec{0}) + \tfrac{1}{2}\vec{R}^0_i\vec{R}^0_i : \vec{\nabla}\vec{\nabla}\vec{s}(\vec{0}) + \cdots. \tag{3.2}$$

Lattice vibrations affect the paramagnetic ion by changing the position of the ion with respect to its neighbors. Thus the displacement field $\vec{s}(\vec{r}, t)$ will appear in the ion-lattice interaction Hamiltonian through the relative displacement

$$\delta\vec{R}_i - \delta\vec{R}_0 = \vec{R}^0_i\cdot\vec{\nabla}\vec{s}(\vec{0}) + \tfrac{1}{2}\vec{R}^0_i\vec{R}^0_i : \vec{\nabla}\vec{\nabla}\vec{s}(\vec{0}). \tag{3.3}$$

Most spin-lattice relaxation processes at low temperatures primarily involve phonons of low energy which are associated with normal modes for which v/ω is much greater than interionic distances. Thus $\mathcal{H}_{11}$ may be restricted to the first term in Eq. (3.3),

$$\delta\vec{R}_i - \delta\vec{R}_0 = \vec{R}^0_i\cdot\vec{\vec{\sigma}}(\vec{0}). \tag{3.4}$$

Almost all previous calculations have employed the assumption (3.4) which is designated the *long-wavelength approximation*. Extension of the following techniques to higher-order terms in (3.3) will be seen to be quite straightforward.

To obtain a "cubic" ion lattice interaction, it is simplest to form linear combinations of strain tensor components at the paramagnetic ion site ($\vec{R}^0_0 = \vec{0}$), transforming as rows of the irreducible representation of the cubic group

$$\sigma_0(n\,\Gamma\beta) = \sum_m \langle n\,m|\,n\,\Gamma\beta\rangle\sigma_{nm}(\vec{0}). \tag{3.5}$$

Using Eq. (2.4), one can write

$$\begin{aligned}
&\sigma_0(0\Gamma_{1g}) = -(1/\sqrt{3})(\sigma_{xx}+\sigma_{yy}+\sigma_{zz}),\\
&\sigma_0(1\Gamma_{4g}1) = \tfrac{1}{2}(\sigma_{zx} - \sigma_{xz} + i\sigma_{zy} - i\sigma_{yz}),\\
&\sigma_0(1\Gamma_{4g}0) = (i/\sqrt{2})(\sigma_{xy} - \sigma_{yx}),\\
&\sigma_0(1\,\Gamma_{4g}-1) = \tfrac{1}{2}(\sigma_{zx} - \sigma_{xz} + i\sigma_{yz} - i\sigma_{zy}),\\
&\sigma_0(2\Gamma_{3g}\theta) = (1/\sqrt{6})(2\sigma_{zz} - \sigma_{xx} - \sigma_{yy}),\\
&\sigma_0(2\Gamma_{3g}\epsilon) = (1/\sqrt{2})(\sigma_{xx} - \sigma_{yy}),\\
&\sigma_0(2\,\Gamma_{5g}1) = \tfrac{1}{2}(\sigma_{xz} + \sigma_{zx} - i\sigma_{yz} - i\sigma_{zy}),\\
&\sigma_0(2\,\Gamma_{5g}0) = (i/\sqrt{2})(\sigma_{xy} + \sigma_{yx}),\\
&\sigma_0(2\,\Gamma_{5g}-1) = \tfrac{1}{2}(\sigma_{xz} + \sigma_{zx} + i\sigma_{yz} + i\sigma_{zy}).
\end{aligned} \tag{3.6}$$

All strain components are evaluated at the origin, $\vec{R}^0_0 = \vec{0}$. Note that the index n is superfluous here (and will be dropped) since Γ, β are sufficient to specify any of the σ_0.

The exact form of the ion operators that will appear in $\mathcal{H}_{11}$ depends on the ion-ligand interaction. Without assuming any model for this interaction at present, but requiring $\mathcal{H}_{11}$ to transform as Γ_{1g}, the ion-lattice Hamiltonian in the long-wavelength approximation must be of the form

$$\mathcal{H}_{11} = \sum_{\Gamma,\beta} c_{\Gamma\beta}\,V(\Gamma\beta)\sigma_0(\Gamma\bar{\beta}), \tag{3.7}$$

in which $V(\Gamma\beta)$ is an ion operator transforming as the βth row of the irreducible representation Γ.

To take full advantage of these symmetry properties, $\sigma_0(\Gamma\beta)$ must be expressed in terms of normal coordinates (2.32). For a spherical-wave expansion,

$$\overleftrightarrow{\sigma}(\vec{0}) = \sum_{Xnmq} s_{Xnmq} \vec{\nabla} \vec{s}_{Xnmq}(\vec{0}), \tag{3.8}$$

and employing (2.26), and the fact that

$$j_l(0) = \delta_{l0}, \tag{3.9}$$

one can show that only $\vec{s}_{L00q}$, $\vec{s}_{M1mq}$, and $\vec{s}_{12mq}$ will make a nonzero contribution to Eq. (3.8). To obtain restricted density-of-states functions for these modes, it is sufficient to realize that (except for a negligible number) these low-angular-momentum modes have little intensity near the boundary and the Bessel functions appearing in the normal modes (2.14), (2.18), and (2.20) can be approximated with the asymptotic form

$$j_n(x) \underset{x\to\infty}{\longrightarrow} (1/x)\cos[x - \tfrac{1}{2}\pi(n+1)]. \tag{3.10}$$

The number $\rho_{L00q}(\omega)$ of normal modes of the form $\vec{s}_{L00q}$ satisfying the boundary condition, with an angular frequency ω^L_{0q} in an interval $d\omega$ about ω can be expressed as

$$\rho_{L00q}(\omega) = R/v_L\pi . \tag{3.11}$$

Similarly, considering the modes $\vec{s}_{M1mq}$ and employing the asymptotic formula (3.10),

$$\rho_{M1mq}(\omega) = R/v_T\pi . \tag{3.12}$$

In applying the asymptotic formula to the boundary conditions for s_{1nmq} modes (2.20), two cases arise. Equation (3.10) indicates that when $j_{n+1}(x) = 0$, then *approximately* $j_{n-1}(x) = 0$. Within this approximation,

$$j_{n+1}[(\omega^1_{2q}/v_T)R] = 0$$

and Eq. (2.20) yields a normalized mode

$$\vec{s}_{12mq} = \left[\tfrac{1}{2}R^3 j_2^2\left(\frac{\omega^1_{2q}}{v_T}R\right)\right]^{-1/2} \times\left[-\sqrt{\tfrac{3}{5}}\vec{Y}_{21m} j_1\left(\frac{\omega^1_{2q}}{v_T}r\right) + \sqrt{\tfrac{2}{5}}\vec{Y}_{23m} j_3\left(\frac{\omega^1_{2q}}{v_T}r\right)\right]. \tag{3.13}$$

On the other hand, if

$$j_{n+1}[(\omega^1_{2q}/v_L)R] = 0,$$

the mode

$$\vec{s}_{12mq} = \left[\tfrac{1}{2}R^3 j_2^2\left(\frac{\omega^1_{2q}}{v_L}R\right)\right]^{-1/2} \times\left[\sqrt{\tfrac{2}{5}}\vec{Y}_{21m} j_1\left(\frac{\omega^1_{2q}}{v_L}r\right) + \sqrt{\tfrac{3}{5}}\vec{Y}_{23m} j_3\left(\frac{\omega^1_{2q}}{v_L}r\right)\right] \tag{3.14}$$

is obtained. But Eq. (3.13) is precisely of the form $\vec{s}_{N2m}$, while Eq. (3.14) is the form $\vec{s}_{L2m}$. Therefore, $\vec{s}_{12m}$ "decomposes" into a nearly longitudinal part $\vec{s}_{L2mq}$ with

$$\rho_{L2m} = R/v_L\pi \tag{3.15}$$

and a nearly transverse part $\vec{s}_{N2mq}$ with

$$\rho_{N2m} = R/v_T\pi . \tag{3.16}$$

Using Eq. (3.10) to evaluate normalization constants, the following normal modes, significant in the ion-lattice interaction, can be written:

$$\vec{s}_{L00q} = \frac{\omega^L_{0q}}{v_L}\left(\frac{2}{R}\right)^{1/2} j_1\left(\frac{\omega^L_{0q}}{v_L}r\right)\vec{Y}_{010}, \tag{3.17a}$$

$$\vec{s}_{M1mq} = i\frac{\omega^M_{2q}}{v_T}\left(\frac{2}{R}\right)^{1/2} j_1\left(\frac{\omega^M_{1q}}{v_T}r\right)\vec{Y}_{11m}, \tag{3.17b}$$

$$\vec{s}_{L2mq} = \frac{\omega^L_{2q}}{v_L}\left(\frac{2}{R}\right)^{1/2}\left[\left(\frac{2}{5}\right)^{1/2} j_1\left(\frac{\omega^L_{2q}}{v_L}r\right)\vec{Y}_{21m} + \left(\frac{3}{5}\right)^{1/2} j_3\left(\frac{\omega^L_{2q}}{v_L}r\right)\vec{Y}_{23m}\right], \tag{3.17c}$$

$$\vec{s}_{N2mq} = \frac{\omega^N_{2q}}{v_T}\left(\frac{2}{R}\right)^{1/2}\left[-\left(\frac{3}{5}\right)^{1/2} j_1\left(\frac{\omega^N_{2q}}{v_T}r\right)\vec{Y}_{21m} + \left(\frac{2}{5}\right)^{1/2} j_3\left(\frac{\omega^N_{2q}}{v_T}r\right)\vec{Y}_{23m}\right]. \tag{3.17d}$$

From these, cubic modes are simply constructed in the usual manner. Specifically,

$$\vec{s}_{L\Gamma_{1g}q} = \frac{\omega^L_q}{v_L}\left(\frac{2}{R}\right)^{1/2} j_1\left(\frac{\omega^L_q}{v_L}r\right)\vec{Y}_{010}, \tag{3.18a}$$

$$\vec{s}_{M\Gamma_{4g}\beta q} = i\frac{\omega^M_q}{v_T}\left(\frac{2}{R}\right)^{1/2} j_1\left(\frac{\omega^M_q}{v_T}r\right) \times\sum_m \langle 1m|1\Gamma_{4g}\beta\rangle\vec{Y}_{11m}, \tag{3.18b}$$

$$\vec{s}_{L\Gamma_{3g}\beta q} = \frac{\omega^L_q}{v_L}\left(\frac{2}{R}\right)^{1/2}\sum_m \langle 2m|2\Gamma_{3g}\beta\rangle \times\left[\left(\frac{2}{5}\right)^{1/2} j_1\left(\frac{\omega^L_q}{v_L}r\right)\vec{Y}_{21m} + \left(\frac{3}{5}\right)^{1/2} j_3\left(\frac{\omega^L_q}{v_L}r\right)\vec{Y}_{23m}\right], \tag{3.18c}$$

$$\vec{s}_{L\Gamma_{5g}\beta q} = \frac{\omega^L_q}{v_L}\left(\frac{2}{R}\right)^{1/2}\sum_m \langle 2m|2\Gamma_{5g}\beta\rangle \times\left[\left(\frac{2}{5}\right)^{1/2} j_1\left(\frac{\omega^L_q}{v_L}r\right)\vec{Y}_{21m} + \left(\frac{3}{5}\right)^{1/2} j_3\left(\frac{\omega^L_q}{v_L}r\right)\vec{Y}_{23m}\right], \tag{3.18d}$$

$$\vec{s}_{N\Gamma_{3g}\beta q} = \frac{\omega^N_q}{v_T}\left(\frac{2}{R}\right)^{1/2}\sum_m \langle 2m|2\Gamma_{3g}\beta\rangle \times\left[-\left(\frac{3}{5}\right)^{1/2} j_1\left(\frac{\omega^N_q}{v_T}r\right)\vec{Y}_{21m}\right.$$

$$+\left(\frac{2}{5}\right)^{1/2} j_3\left(\frac{\omega_q^N}{v_T} r\right) \vec{\Upsilon}_{23m}\Big], \qquad (3.18e)$$

$$\vec{s}_{N\,\Gamma_{5g}\beta\,q} = \frac{\omega_q^N}{v_T}\left(\frac{2}{R}\right)^{1/2} \sum_m \langle 2m | 2\Gamma_{5g}\beta\rangle \times \left[-\left(\frac{3}{5}\right)^{1/2} j_1\left(\frac{\omega_q^N}{v_T} r\right) \vec{\Upsilon}_{21m} + \left(\frac{2}{5}\right)^{1/2} j_3\left(\frac{\omega_q^N}{v_T} r\right) \vec{\Upsilon}_{23m}\right]. \qquad (3.18f)$$

For conciseness, the angular-momentum index n has been dropped. Introducing creation and annihilation operators (2.36) the strain components (3.6) may then be written

$$\sigma_0(\Gamma_{1g}) = -i\left(\frac{\hbar}{12\pi\rho R}\right)^{1/2} \times \sum_q \frac{(\omega_q^L)^{3/2}}{v_L^2}\left(a^\dagger_{L\,\Gamma_{1g}q} - a_{L\,\Gamma_{1g}q}\right), \qquad (3.19a)$$

$$\sigma_0(\Gamma_{4g}\beta) = -i\left(\frac{\hbar}{12\pi\rho R}\right)^{1/2} \times \sum_q \frac{(\omega_q^M)^{3/2}}{v_T^2}\left(a^\dagger_{M\,\Gamma_{4g}\beta\,q} - c_{\Gamma_{4g}\beta} a_{M\,\Gamma_{4g}\bar{\beta}\,q}\right), \qquad (3.19b)$$

$$\sigma_0(\Gamma_{3g}\beta) = -i\left(\frac{\hbar}{12\pi\rho R}\right)^{1/2} \times \sum_q \left[\left(\frac{2}{5}\right)^{1/2} \frac{(\omega_q^L)^{3/2}}{v_L^2}\left(a^\dagger_{L\,\Gamma_{3g}\beta\,q} - c_{\Gamma_{3g}\beta} a_{L\,\Gamma_{3g}\bar{\beta}\,q}\right) - \left(\frac{3}{5}\right)^{1/2} \frac{(\omega_q^N)^{3/2}}{v_T^2}\left(a_{N\,\Gamma_{3g}\beta\,q} - c_{\Gamma_{3g}\beta} a_{N\,\Gamma_{3g}\bar{\beta}\,q}\right)\right], \qquad (3.19c)$$

$$\sigma_0(\Gamma_{5g}\beta) = -i\left(\frac{\hbar}{12\pi\rho R}\right)^{1/2} \times \sum_q \left[\left(\frac{2}{5}\right)^{1/2} \frac{(\omega_q^L)^{3/2}}{v_L^2}\left(a^\dagger_{L\,\Gamma_{5g}\beta\,q} - c_{\Gamma_{5g}\beta} a_{L\,\Gamma_{5g}\bar{\beta}\,q}\right) - \left(\frac{3}{5}\right)^{1/2} \frac{(\omega_q^N)^{3/2}}{v_T^2}\left(a^\dagger_{N\,\Gamma_{5g}\beta\,q} - c_{\Gamma_{5g}\beta} a_{N\,\Gamma_{5g}\bar{\beta}\,q}\right)\right]. \qquad (3.19d)$$

Matrix elements of the $\sigma_0(\Gamma\beta)$ will appear in transition-rate expressions in the forms

$$|\langle N_{X\,\Gamma\bar{\beta}\,q}|\sigma_0(\Gamma\bar{\beta})|N_{X\,\Gamma\bar{\beta}\,q} - 1\rangle|^2,$$

$$|\langle N_{X\,\Gamma\beta\,q}|\sigma_0(\Gamma\bar{\beta})|N_{X\,\Gamma\beta\,q} + 1\rangle|^2,$$

$$|\langle N_{X\,\Gamma\beta\,q}|\sigma_0(\Gamma\beta)|N_{X\,\Gamma\beta\,q} - 1\rangle|^2,$$

$$|\langle N_{X\,\Gamma\bar{\beta}\,q}|\sigma_0(\Gamma\beta)|N_{X\,\Gamma\bar{\beta}\,q} + 1\rangle|^2,$$

which are actually independent of β, and (abbreviating)

$$|\langle N_{X\Gamma q}|\sigma_0(\Gamma)|N_{X\Gamma q} - 1\rangle|^2 = \frac{C(X,\Gamma)}{v_X^4}\frac{\hbar}{12\pi\rho R}(\omega_q^X)^3 N_{X\Gamma q}, \qquad (3.20a)$$

$$|\langle N_{X\Gamma q}|\sigma_0(\Gamma)|N_{X\Gamma q} + 1\rangle|^2 = \frac{C(X,\Gamma)}{v_X^4}\frac{\hbar}{12\pi\rho R}(\omega_q^X)^3 (N_{X\Gamma q} + 1), \qquad (3.20b)$$

with $C(L,\Gamma_{1g}) = C(M,\Gamma_{4g}) = 1$, $C(L,\Gamma_{3g}) = C(L,\Gamma_{5g}) = \frac{2}{5}$, and $C(N,\Gamma_{3g}) = C(N,\Gamma_{5g}) = \frac{3}{5}$.

A. Relaxation in a multilevel system with degenerate levels

Spin-lattice relaxation rates will be presented in a form suitable for calculation of the time evolution of a system which has many levels of non-negligible population. Assuming the lattice remains in a thermal-equilibrium state, ion transition rates between two states $|i\rangle$ and $|j\rangle$ will obey the thermodynamic relationship

$$W_{i\to j}/W_{j\to i} = e^{(E_i - E_j)/kT}. \qquad (3.21)$$

Thus, the transition rate between the two states may be concisely expressed in a symmetric direction-corrected rate

$$T^{ij} = W_{i\to j}\, e^{(E_j - E_i)/2kT}. \qquad (3.22)$$

The hyperfine systems to be studied are characterized by a set of degenerate energy levels at zero field, whose degeneracy is removed by an external magnetic field. In the zero-field situation, with degenerate levels present, the quantity of more direct experimental interest is the level-to-level transition rate

$$W^{\text{lev}}_{k\to l} = \sum_{\substack{i\in k \\ j\in l}} \frac{W_{i\to j}}{g_k}, \qquad (3.23)$$

where k and l are energy *levels*, $|i\rangle$ and $|j\rangle$ are states within these levels, and g_k is the degeneracy of level k. The population P_k of the kth energy level obeys the kinetic equation

$$\frac{dP_k}{dt} = \sum_l \left(-W^{\text{lev}}_{k\to l} P_k + W^{\text{lev}}_{l\to k} P_l\right), \qquad (3.24)$$

which may be cast into matrix form

$$\frac{d\underline{P}}{dt} = \underline{W}^{\text{lev}}\underline{P}, \qquad (3.25)$$

in which $\underline{P}$ is a vector with components P_k and $\underline{W}^{\text{lev}}$ is the level-to-level *trasition-rate matrix* given by

$$W^{\text{lev}}_{kl} = W^{\text{lev}}_{l\to k} \quad (k \neq l), \qquad W^{\text{lev}}_{kk} = -\sum_l W^{\text{lev}}_{k\to l}. \qquad (3.26)$$

$\underline{W}$ itself is not symmetric and it is more convenient to work with the scaled symmetric (*reduced-transition rate*) matrix

$$\underline{\tilde{W}}^{\text{lev}} = \underline{U}\,\underline{W}^{\text{lev}}\underline{U}^{-1} . \tag{3.27}$$

U is a diagonal matrix with

$$U_{kk} = (1/\sqrt{g_k})\, e^{(E_k - E_{\text{ref}})/2kT} \tag{3.28}$$

in which E_{ref} is any convenient reference energy. The symmetric matrix element $\tilde{W}_{kl}^{\text{lev}}$ is the analog, for a system with degenerate levels, of the state-to-state symmetrized rate T^{ij}. Computed values of $\underline{\tilde{W}}^{\text{lev}}$ will thus be given for the zero-field case and values of $T^{ij}(\underline{T})$ for systems at nonzero field. Given $\underline{\tilde{W}}^{\text{lev}}$, the time evolution of $\underline{P}$ may be obtained as described earlier.[9]

For a two-level nondegenerate system there will be only a single rate T^{12}, and one might prefer to speak of the conventional relaxation time defined by the relationship

$$1/T_1 = 2T^{12}\cosh[(E_2 - E_1)/2kT] \approx 2T^{12} \tag{3.29}$$

as long as $|E_2 - E_1| \ll kT$.

In Sec. III B–III D, general rate formulas for the various relaxation mechanisms will be given in terms of $\underline{T}$, which can be simply related to $\underline{\tilde{W}}^{\text{lev}}$ in the zero-field degenerate situation by the above formalism.

B. Direct process

Consider first the rate at which paramagnetic ions undergo a transition from state $|j\rangle$ to a lower-lying state $|i\rangle$ accompanied by emission of a single phonon in the mode $\vec{s}_{X\Gamma\beta q}$ with energy conservation (direct process). Using the Golden Rule of time-dependent perturbation theory this rate can be written

$$\begin{aligned} W_{j\to i} &= (2\pi/\hbar)\left|\langle jN_{X\Gamma\beta q}\left|\mathcal{H}_{11}\right|iN_{X\Gamma\beta q}+1\rangle\right|^2 \\ &\quad\times\delta(E_j - E_i - \hbar\omega_q^X) \\ &= (2\pi/\hbar)\left|\langle j\left|V(\Gamma\beta)\right|i\rangle\right|^2 \\ &\quad\times\left|\langle N_{X\Gamma\beta q}\left|\sigma_0(\Gamma\bar{\beta})\right|N_{X\Gamma\beta q}+1\rangle\right|^2 \\ &\quad\times\delta(E_j - E_i - \hbar\omega_q^X) . \end{aligned} \tag{3.30}$$

To obtain an expression for the total rate at which the ion transition occurs, this expression is summed over all normal modes of the lattice. Using the restricted density of states [Eqs. (3.11), (3.12), (3.15), and (3.16)] the conversion

$$\sum_q \to \frac{R}{v_X \pi}\int d\omega_q^X$$

for each branch is possible. If it is further assumed that all the lattice normal modes are at their thermal equilibrium population, so that

$$N = (e^{(E_j - E_i)/kT} - 1)^{-1} ,$$

it follows that

$$W_{j\to i}^{\text{direct}} = \frac{1}{6\pi\rho h}\left(\frac{E_j - E_i}{\hbar}\right)^3 \frac{e^{(E_j-E_i)/kT}}{e^{(E_j-E_i)/kT}-1} \times\sum_{X\Gamma}\frac{C(X,\Gamma)}{v_X^5}\sum_\beta\left|\langle j\left|V(\Gamma\beta)\right|i\rangle\right|^2 . \tag{3.31}$$

In general the $V(\Gamma_{1g})$ term is deleted as it does not contribute to the relaxation. Note that (3.31) is equivalent to the result of Van Vleck[4,5] obtained by "averaging over all polarizations and directions of propagation" for plane wave phonons.

The transition rate (3.30) corresponds to a symmetrized rate

$$T_{\text{direct}}^{ij} = \frac{1}{12\pi\rho\hbar}\left(\frac{E_j - E_i}{\hbar}\right)^3 \text{cosech}\left(\frac{E_j - E_i}{2kT}\right) \times\sum_{X\Gamma}\frac{C(X,\Gamma)}{v_X^5}\sum_\beta\left|\langle j\left|V(\Gamma\beta)\right|i\rangle\right|^2 , \tag{3.32}$$

which becomes, in the limit $|E_j - E_i|/kT \ll 1$,

$$T_{\text{direct}}^{ij} = \frac{kT(E_j - E_i)^2}{6\pi\rho\hbar^4}\sum_{X\Gamma}\frac{C(X\Gamma)}{v_X^5}\sum_\beta\left|\langle j\left|V(\Gamma\beta)\right|i\rangle\right|^2 , \tag{3.33}$$

displaying a characteristic linear dependence on temperature.

C. Raman process

The direct process is the dominant relaxation mechanism at low temperature in the familiar high-field situation but at about $2K$ multiphonon processes typically dominate. In order to account for observed temperature dependences, second-order perturbation theory is invoked, allowing two-phonon processes for which the difference in phonon energies equals the separation of the energy levels involved. The second-order operator can be represented as

$$V_{\text{eff}} = \sum_\tau \frac{\mathcal{H}_{11}|\tau\rangle\langle\tau|\mathcal{H}_{11}}{E_0 - E_\tau} , \tag{3.34}$$

in which the summation runs over all intermediate states of the combined ion-lattice system. Since the separation in energy of initial and final states is usually quite small, the possibility of creating or destroying two phonons in a transition may be neglected. For a general transition of the form

$$|j, N_{X_1\Gamma_1\beta_1 q_1}, N_{X_2\Gamma_2\beta_2 q_2}\rangle \to |i, N_{X_1\Gamma_1\beta_1 q_1} - 1, N_{X_2\Gamma_2\beta_2 q_2}+1\rangle , \tag{3.35}$$

the transition rate can be written

$$W = \frac{2\pi}{\hbar}\left|\sum_t\left(\frac{\langle j, N_{X_1\Gamma_1\beta_1 q_1}\,|\,V(\Gamma_1\bar{\beta}_1)\sigma_0(\Gamma_1\beta_1)\,|\,t, N_{X_1\Gamma_1\beta_1 q_1}-1\rangle}{E_j - E_t + \hbar\omega_{q_1}^{X_1}}\right.\right.$$

$$\times\langle t, N_{X_2\Gamma_2\beta_2 q_2}|\,V(\Gamma_2\beta_2)\sigma_0(\Gamma_2\bar{\beta}_2)\,|\,i, N_{X_2\Gamma_2\beta_2 q_2}+1\rangle + \frac{\langle j, N_{X_2\Gamma_2\beta_2 q_2}|\,V(\Gamma_2\beta_2)\sigma_0(\Gamma_2\bar{\beta}_2)\,|\,t, N_{X_2\Gamma_2\beta_2 q_2}+1\rangle}{E_j - E_t - \hbar\omega_{q_2}^{X_2}}$$

$$\left.\left.\times\langle t, N_{X_1\Gamma_1\beta_1 q_1}|\,V(\Gamma_1\bar{\beta}_1)\sigma_0(\Gamma_1\beta_1)\,|\,i, N_{X_1\Gamma_1\beta_1 q_1}-1\rangle\right)\right|^2 \delta(E_j - E_i + \hbar\omega_{q_1}^{X_1} - \hbar\omega_{q_2}^{X_2})$$

$$= \frac{2\pi}{\hbar}\left|\sum_t\left(\frac{\langle j\,|\,V(\Gamma_1\bar{\beta}_1)\,|\,t\rangle\langle t|\,V(\Gamma_2\beta_2)\,|\,i\rangle}{E_j - E_t + \hbar\omega_{q_1}^{X}} + \frac{\langle j\,|\,V(\Gamma_2\beta_2)\,|\,t\rangle\langle t|\,V(\Gamma_1\bar{\beta}_1)\,|\,i\rangle}{E_j - E_t - \hbar\omega_{q_2}^{X_2}}\right)\right|^2$$

$$\times\left|\langle N_{X_1\Gamma_1\beta_1 q_1}\,|\,\sigma_0(\Gamma_1\beta_1)\,|\,N_{X_1\Gamma_1\beta_1 q_1}-1\rangle\right|^2\left|\langle N_{X_2\Gamma_2\beta_2 q_2}|\,\sigma_0(\Gamma_2\bar{\beta}_2)\,|\,N_{X_2\Gamma_2\beta_2 q_2}+1\rangle\right|^2\delta(E_j - E_i + \hbar\omega_{q_1}^{X_1} - \hbar\omega_{q_2}^{X_2})\,. \tag{3.36}$$

Summing over all possible final states, the above becomes

$$W_{j\to i}^{\text{Raman}} = \frac{2\pi}{\hbar}\sum_{X_1X_2}\int_0^{\omega_{\max}^{X_1}}\frac{R}{v_{X_1}\pi}\,d\omega_1\int_0^{\omega_{\max}^{X_2}}\frac{R}{v_{X_2}\pi}\,d\omega_2$$

$$\times\sum_{\Gamma_1\Gamma_2}\left|\langle N_{X_1\Gamma_1 q_1}|\,\sigma_0(\Gamma_1)\,|\,N_{X_1\Gamma_1 q_1}-1\rangle\right|^2\left|\langle N_{X_2\Gamma_2 q_2}|\,\sigma_0(\Gamma_2)\,|\,N_{X_2\Gamma_2 q_2}+1\rangle\right|^2$$

$$\times\sum_{\beta_1\beta_2}\left|\sum_t\left(\frac{\langle j\,|\,V(\Gamma_1\bar{\beta}_1)\,|\,t\rangle\langle t|\,V(\Gamma_2\beta_2)\,|\,i\rangle}{E_j - E_t + \hbar\omega_1}\right.\right.$$

$$\left.\left.+\frac{\langle j\,|\,V(\Gamma_2\beta_2)\,|\,t\rangle\langle t|\,V(\Gamma_1\bar{\beta}_1)\,|\,i\rangle}{E_j - E_t - \hbar\omega_2}\right)\right|^2\delta(E_j - E_i + \hbar\omega_1 - \hbar\omega_2)\,. \tag{3.37}$$

The transition rate depends critically on the ion excited states $|t\rangle$ and their energies. We postpone discussion of resonant processes characterized by a vanishing denominator in (3.34) or (3.36) and consider presently nonresonant processes. Energy terms appearing in (3.37) are characteristically of three different orders of magnitude with hyperfine and Zeeman energies $\ll$ thermal energies $\ll$ crystal-field energies. The major contribution to Raman relaxation is attributed to phonons of energy $\hbar\omega \approx kT$ so that hyperfine-energy terms in (3.37) may be neglected in comparison with $\hbar\omega$. The somewhat simpler form

$$W_{j\to i}^{\text{Raman}} = \frac{e^{(E_j - E_i)/2kT}}{288\pi^3\rho^2}\sum_{X_1X_2}\sum_{\Gamma_1\Gamma_2}\frac{C(X_1\Gamma_1)}{v_{X_1}^5}\,\frac{C(X_2\Gamma_2)}{v_{X_2}^5}\int_0^\infty\omega^6\,\text{cosech}^2\frac{\hbar\omega}{2kT}\,d\omega$$

$$\times\sum_{\beta_1\beta_2}\left|\sum_t\left(\frac{\langle j|\,V(\Gamma_1\bar{\beta}_1)\,|\,t\rangle\langle t|\,V(\Gamma_2\beta_2)\,|\,i\rangle}{-\Delta_t + \hbar\omega} + \frac{\langle j\,|\,V(\Gamma_2\beta_2)\,|\,t\rangle\langle t|\,V(\Gamma_1\bar{\beta}_1)\,|\,i\rangle}{-\Delta_t - \hbar\omega}\right)\right|^2 \tag{3.38}$$

is obtained, in which

$$\Delta_t = E_t - E_j$$

and the integration with respect to ω has been extended to infinity with negligible error.

In many typical systems the paramagnetic ion possesses a number of Zeeman or hyperfine states, with energies much smaller than kT separated from the first set of excited states by an energy much larger than kT. In such a case the sum over intermediate states t in (3.38) may be separated into a sum over low-lying states t_l with energies $\ll kT$ and a set of excited states t_h with energies $\gg kT$. Neglecting Δ_{t_l} with respect to $\hbar\omega$ in (3.38), one obtains

$$T_{\text{Raman}}^{ij} = T_{R5}^{ij} + T_{R6}^{ij} + T_{R7}^{ij} + T_{R8}^{ij} + T_{R9}^{ij}\,, \tag{3.39}$$

with

$$T_{RN}^{ij} = \frac{1}{288\pi^3\rho^2}\sum_{X_1X_2}\sum_{\Gamma_1\Gamma_2}\frac{C(X_1\Gamma_1)}{v_{X_1}^5}\,\frac{C(X_2\Gamma_2)}{v_{X_2}^5}\sum_{\beta_1\beta_2}I_N\,V_N(\Gamma_1\beta_1, \Gamma_2\beta_2)\,. \tag{3.40}$$

In Eq. (3.40) the lattice integral I_N is given by

$$I_N = \int_0^\infty \omega^{N-1} \operatorname{cosech}^2\left(\frac{\hbar\omega}{2kT}\right) d\omega \,, \tag{3.41}$$

or explicitly[20]

$$I_5 = \frac{16\pi^4}{15}\left(\frac{kT}{\hbar}\right)^5, \quad I_6 = 497.7\left(\frac{kT}{\hbar}\right)^6, \quad I_7 = \frac{64\pi^6}{21}\left(\frac{kT}{\hbar}\right)^7, \quad I_8 = 20\,328\left(\frac{kT}{\hbar}\right)^8, \quad I_9 = \frac{256\pi^8}{15}\left(\frac{kT}{\hbar}\right)^9,$$

while the ion terms $V_N(\Gamma_1\beta_1, \Gamma_2\beta_2)$ are given by

$$V_5(\Gamma_1\beta_1, \Gamma_2\beta_2) = \frac{1}{\hbar^2}\left|\sum_{t_l} [\langle j|V(\Gamma_1\bar\beta_1)|t_l\rangle\langle t_l|V(\Gamma_2\beta_2)|i\rangle - \langle j|V(\Gamma_2\beta_2)|t_l\rangle\langle t_l|V(\Gamma_1\bar\beta_1)|i\rangle]\right|^2,$$

$$V_6(\Gamma_1\beta_1, \Gamma_2\beta_2) = \frac{-2}{\hbar}\sum_{t_l}[\langle j|V(\Gamma_1\bar\beta_1)|t_l\rangle\langle t_l|V(\Gamma_2\beta_2)|i\rangle - \langle j|V(\Gamma_2\beta_2)|t_l\rangle\langle t_l|V(\Gamma_1\bar\beta_1)|i\rangle]$$
$$\times\sum_{t_h}\left(\frac{\langle j|V(\Gamma_1\bar\beta_1)|t_h\rangle\langle t_h|V(\Gamma_2\beta_2)|i\rangle}{\Delta_{t_h}} + \frac{\langle j|V(\Gamma_2\beta_2)|t_h\rangle\langle t_h|V(\Gamma_1\bar\beta_1)|i\rangle}{\Delta_{t_h}}\right),$$

$$V_7(\Gamma_1\beta_1, \Gamma_2\beta_2) = \left|\sum_{t_h}\left(\frac{\langle j|V(\Gamma_1\bar\beta_1)|t_h\rangle\langle t_h|V(\Gamma_2\beta_2)|i\rangle}{\Delta_{t_h}} + \frac{\langle j|V(\Gamma_2\beta_2)|t_h\rangle\langle t_h|V(\Gamma_1\bar\beta_1)|i\rangle}{\Delta_{t_h}}\right)\right|^2,$$

$$V_8(\Gamma_1\beta_1, \Gamma_2\beta_2) = 2\hbar\sum_{t_h}\left(\frac{\langle j|V(\Gamma_1\bar\beta_1)|t_h\rangle\langle t_h|V(\Gamma_2\beta_2)|i\rangle}{\Delta_{t_h}} + \frac{\langle j|V(\Gamma_2\beta_2)|t_h\rangle\langle t_h|V(\Gamma_1\bar\beta_1)|i\rangle}{\Delta_{t_h}}\right)$$
$$\times\sum_{t_h'}\left(\frac{\langle j|V(\Gamma_1\bar\beta_1)|t_h'\rangle\langle t_h'|V(\Gamma_2\beta_2)|i\rangle}{\Delta_{t_h'}^2} - \frac{\langle j|V(\Gamma_2\beta_2)|t_h'\rangle\langle t_h'|V(\Gamma_1\bar\beta_1)|i\rangle}{\Delta_{t_h'}^2}\right),$$

$$V_9(\Gamma_1\beta_1, \Gamma_2\beta_2) = \hbar^2\left|\sum_{t_h}\left(\frac{\langle j|V(\Gamma_1\bar\beta_1)|t_h\rangle\langle t_h|V(\Gamma_2\beta_2)|i\rangle}{\Delta_{t_h}^2} - \frac{\langle j|V(\Gamma_2\beta_2)|t_h\rangle\langle t_h|V(\Gamma_1\bar\beta_1)|i\rangle}{\Delta_{t_h}^2}\right)\right|^2.$$

In the usual case studied in high-field paramagnetic resonance, $|i\rangle$ and $|j\rangle$ are conjugate electronic states under time reversal, and the ion matrix elements have the property

$$\langle j|V(\Gamma_2\beta_2)|t\rangle\langle t|V(\Gamma_1\beta_1)|i\rangle = -\langle j|V(\Gamma_1\beta_1)|\bar t\rangle\langle\bar t|V(\Gamma_2\beta_2)|i\rangle \tag{3.42a}$$

if the electronic angular momentum is half-odd-integral, and

$$\langle j|V(\Gamma_2\beta_2)|t\rangle\langle t|V(\Gamma_1\beta_1)|i\rangle = \langle j|V(\Gamma_1\beta_1)|\bar t\rangle\langle\bar t|V(\Gamma_2\beta_2)|i\rangle \tag{3.42b}$$

if the electronic angular momentum is integral. [Since $V(\Gamma\beta)$ affects only the electronic coordinates, the same identities (3.42) apply when $|i\rangle$ and $|j\rangle$ are direct products of electronic time conjugate states with the same nuclear state; the *electronic* angular momentum thus determines whether (3.42a) or (3.42b) applies.] Equation (3.42a) gives rise to the familiar Van Vleck cancellation. Since the energy separation of $|t\rangle$ and $|\bar t\rangle$ (if any) is negligible compared to thermal energies, the Raman rates (3.38) and (3.39) simplify considerably if $|i\rangle$ and $|j\rangle$ are conjugate states.

For a system of half-odd-integral angular momentum (Kramers system), Raman relaxation between conjugate states displays a characteristic T^5 temperature dependence[21] (if a second low-lying Kramers doublet exists) together with a T^9 dependence.[2] In this case, the simplified forms

$$T_{R5}^{ij} = \frac{2\pi}{135\rho^2\hbar^2}\left(\frac{kT}{\hbar}\right)^5\sum_{X_1X_2}\sum_{\Gamma_1\Gamma_2}\frac{C(X_1\Gamma_1)}{v_{X_1}^5}\frac{C(X_2\Gamma_2)}{v_{X_2}^5}$$
$$\times\sum_{\beta_1\beta_2}\left|\sum_{t_l}\langle j|V(\Gamma_1\beta_1)|t_l\rangle\langle t_l|V(\Gamma_2\beta_2)|i\rangle\right|^2, \tag{3.43}$$

$$T_{R9}^{ij} = \frac{32\pi^5\hbar^2}{135\rho^2}\left(\frac{kT}{\hbar}\right)^9\sum_{X_1X_2}\sum_{\Gamma_1\Gamma_2}\frac{C(X_1\Gamma_1)}{v_{X_1}^5}\frac{C(X_2\Gamma_2)}{v_{X_2}^5}$$
$$\times\sum_{\beta_1\beta_2}\left|\sum_{t_h}\{[\langle j|V(\Gamma_1\beta_1)|t_h\rangle \times\langle t_h|V(\Gamma_2\beta_2)|i\rangle]/\Delta_{t_h}^2\}\right|^2 \tag{3.44}$$

are obtained.

For a system of integral angular momentum, Raman relaxation between conjugate states displays a characteristic T^7 temperature dependence.

In this case (3.39) simplifies to

$$T^{ij}_{R7}=\frac{8\pi^3}{189\rho^2}\left(\frac{kT}{\hbar}\right)^7\sum_{X_1X_2}\sum_{\Gamma_1\Gamma_2}\frac{C(X_1\Gamma_1)}{v^5_{X_1}}\frac{C(X_2\Gamma_2)}{v^5_{X_2}}\times\sum_{\beta_1\beta_2}\left|\sum_{t_h}\{[\langle j|V(\Gamma_1\beta_1)|t_h\rangle\times\langle t_h|V(\Gamma_2\beta_2)|i\rangle]/\Delta_t\}\right|^2. \quad (3.45)$$

For a transition between states *not* conjugate under time reversal all terms in (3.39) will in general be nonzero and a complicated temperature dependence results. It is shown in Sec. V that matrix elements between hyperfine levels derived from a Kramers doublet actually satisfy the identity (3.42a) owing to the assumption that $V(\Gamma\beta)$ acts only on the electronic coordinates. Relaxation in such a system is therefore characterized by a T^9 dependence. It is also shown that Raman relaxation among hyperfine states derived from a Γ_8 quartet Kramers electronic level involves in general T^5 through T^9 terms.

D. Resonant-Raman (Orbach) process

To complete discussion of relaxation processes associated with the two-phonon Hamiltonian (3.34), it is necessary to consider what occurs when the lattice possesses normal modes such that

$$\hbar\omega=E_t-E_j\ ,$$

for which the first energy denominator in Eq. (3.36) vanishes. Following Orbach[2] the term $\frac{1}{2}i\Gamma_t$ is added to that denominator, such that Γ_t is the linewidth of the excited state $|t\rangle$ given by

$$\Gamma_t=\sum_k\frac{1}{6\pi\rho}\left(\frac{E_t-E_k}{\hbar}\right)^3\frac{e^{(E_t-E_k)/kT}}{e^{(E_t-E_k)/kT}-1}\times\sum_{X\Gamma\beta}\frac{C(X\Gamma)}{v^5_X}|\langle t|V(\Gamma\beta)|k\rangle|^2\ . \quad (3.46)$$

k runs over all lower-lying ion states.[22] The resonant-Raman (Orbach) contribution to the direction-corrected rate is then

$$T^{ij}_{\text{Orbach}}=\frac{1}{144\pi^2\rho^2\hbar}\sum_t\left(\frac{\Delta_t}{\hbar}\right)^6\frac{\operatorname{cosech}^2(\Delta_t/2kT)}{\Gamma_t}\times\sum_{X_1X_2}\sum_{\Gamma_1\Gamma_2}\frac{C(X_1\Gamma_1)}{v^5_{X_1}}\frac{C(X_2\Gamma_2)}{v^5_{X_2}}\times\sum_{\beta_1\beta_2}|\langle j|V(\Gamma_1\beta_1)|t\rangle\times\langle t|V(\Gamma_2\beta_2)|i\rangle|^2\ . \quad (3.47)$$

If, as is usually the case, almost the entire linewidth of $|t\rangle$ may be attributed to states $|k\rangle$ with nearly the same energy as $|j\rangle$, we obtain the far simpler form

$$T^{ij}_{\text{Orbach}}=\frac{1}{6\pi\rho\hbar}\sum_t\left(\frac{\Delta_t}{\hbar}\right)^3\times\left(\left(e^{\Delta_t/kT}-1\right)\sum_{X\Gamma\beta}\frac{C(X\Gamma)}{v^5_X}|\langle t|V(\Gamma\beta)|k\rangle|^2\right)^{-1}\times\sum_{X_1X_2}\sum_{\Gamma_1\Gamma_2}\frac{C(X_1\Gamma_1)}{v^5_{X_1}}\frac{C(X_2\Gamma_2)}{v^5_{X_2}}\times\sum_{\beta_1\beta_2}|\langle j|V(\Gamma_1\beta_1)|t\rangle\times\langle t|V(\Gamma_2\beta_2)|i\rangle|^2\ . \quad (3.48)$$

In the region $\Delta_t\gg kt$, we have the characteristic $e^{-\Delta_t/kT}$ temperature dependence.

While the direct and Raman processes characteristically involve low-energy long-wavelength phonons, the Orbach process usually involves high-energy short-wavelength lattice modes and does not fit well with the long-wavelength approximation and the continuum model in general. It is therefore expected that resonant-Raman relaxation rates will be somewhat less reliable than those for the direct and Raman processes, yet we feel that these rates too will be of considerable qualitative and heuristic value.

IV. ELECTRONIC AND HYPERFINE LEVELS

The ground and first-excited levels of the ions Tm^{2+}, Ho^{2+}, and Er^{3+} and their energy separation are given in Table I. As is usually the case for lanthanide ions, the spin-orbit interaction $\xi(r)\vec{L}\cdot\vec{S}$ is much larger than the crystal field $\mathcal{H}_{cf}$ so that J, the total electronic angular momentum, is approximately a good quantum number, even in a nonspherical crystal environment. At a cubic site the crystal-field Hamiltonian takes on a particularly simple form

$$\mathcal{H}_{cf}=A_4\langle r^4\rangle\langle J\|\beta\|J\rangle[O^0_4(J)+5O^4_4(J)]+A_6\langle r^6\rangle\langle J\|\gamma\|J\rangle[O^0_6(J)-21O^4_6(J)]\ . \quad (4.1)$$

O^m_n and $\langle J\|\chi\|J\rangle$ are the conventional operator equivalents and proportionality factors tabulated by Abragam and Bleaney.[23]

The quantities $A_4\langle r^4\rangle$ and $A_6\langle r^6\rangle$ are typically obtained from experimentally derived spectroscopic data. A_4 and A_6 could be calculated from some

TABLE I. Ground and first-excited levels of the free ions Tm^{2+}, Ho^{2+}, Er^{3+}.

Ion	Configuration	Ground level	First excited level	Separation (cm^{-1})
Tm^{2+}	$4f^{13}$	$^2F_{7/2}$	$^2F_{5/2}$	9000[a]
Ho^{2+}	$4f^{11}$	$^4I_{15/2}$	$^4I_{13/2}$	5500[b]
Er^{3+}	$4f^{11}$	$^4I_{15/2}$	$^4I_{13/2}$	6500[c]

[a]Reference 25.
[b]Reference 33.
[c]Reference 23, p. 284.

TABLE II. Crystal-field and free-ion parameters for the systems studied (see Sec. IV).

Parameter	$CaF_2:{}^{169}Tm^{2+}$ [a]	$CaF_2:{}^{165}Ho^{2+}$	$MgO:{}^{167}Er^{3+}$
$A_4\langle r^4\rangle$ (cm^{-1})	180	295	442
$A_6\langle r^6\rangle$ (cm^{-1})	−34.7	−28.9	16.8
$\langle r^2\rangle$ (Å^2)	0.204	0.214	0.187
$\langle r^4\rangle$ (Å^4)	0.336	0.524	0.178
$\langle r^6\rangle$ (Å^6)	0.787	0.845	0.279
g_J	1.151	−1.182	1.2
a(MHz)	−367.125	779.7	−87.0
I	$\frac{1}{2}$	$\frac{7}{2}$	$\frac{7}{2}$

[a]Calculations for the direct process in $SrF_2:Tm^{2+}$, discussed briefly in Sec. IV A, assume identical values for $\langle r^n\rangle$. Dynamical crystal-field parameters were calculated from a point-charge model for the SrF_2 lattice and hyperfine admixtures of excited states were computed using the observed energy of the Γ_8 electronic level (Ref. 31).

model (i.e., point charges) and $\langle r^4\rangle$ and $\langle r^6\rangle$ viewed as phenomenological parameters or alternatively *ab initio* (Hartree-Fock[24]) values of $\langle r^4\rangle$ and $\langle r^6\rangle$ might be employed and A_4 and A_6 viewed as parameters. In constructing an ion-lattice Hamiltonian, the electron-nucleus separation expectation values $\langle r^2\rangle$, $\langle r^4\rangle$, and $\langle r^6\rangle$ are also required. The ion-lattice Hamiltonian will be derived from a point-charge model since insufficient experimental data are available for direct determination of all "dynamic-crystal-field" parameters. For internal consistency phenomenological values of $\langle r^4\rangle$ and $\langle r^6\rangle$ must then be employed. Since $\langle r^2\rangle$ is not obtainable from spectroscopic measurements, however, the Hartree-Fock value of this parameter must be chosen. Tables II and III contain parameters used in this calculation. The energy levels of a Kramers ion at a cubic site are split into site states transforming as irreducible representations Γ_6, Γ_7 (doublets), and Γ_8 (quartet) of the cubic double group O^*. The lowest electronic levels of the systems chosen for study, $CaF_2:Tm^{2+}$, $CaF_2:Ho^{2+}$, and $MgO:Er^{3+}$ are Γ_6, Γ_7, and Γ_8, respectively. Wave functions and energy levels of the ground and lower-excited electronic levels of the systems are given in Table IV.

Within a manifold of constant J the Zeeman and hyperfine interactions for the free ion have the form

$$\mathcal{H}_J = g_J\mu_B\vec{H}\cdot\vec{J} + a\vec{I}\cdot\vec{J} + g_n'\mu_N\vec{H}\cdot\vec{I} + \mathcal{H}_{quad}\,, \quad (4.2)$$

where the quadrupole term is of the form

$$\begin{aligned}\mathcal{H}_{quad} = P_{quad}\{&[3J_z^2 - J(J+1)][3I_z^2 - I(I+1)]\\ &+\tfrac{3}{2}[(J_zJ_+ + J_+J_z)(I_zI_- + I_-I_z)\\ &+(J_zJ_- + J_-J_z)(I_zI_+ + I_+I_z)]\\ &+\tfrac{3}{2}(J_+^2I_-^2 + J_-^2I_+^2)\}\,.\end{aligned}$$

Zeeman and hyperfine parameters for the systems studied are also included in Table II.

For a Γ_6 or Γ_7 doublet, the lowest hyperfine multiplet can be characterized by the spin Hamiltonian

$$\mathcal{H}_s = g\mu_B\vec{H}\cdot\vec{\tilde{S}} + A\vec{I}\cdot\vec{\tilde{S}} + g_n\mu_N\vec{H}\cdot\vec{I}\,, \quad (4.3)$$

with the fictitious spin $\tilde{S} = \frac{1}{2}$ and

$$g/g_J = A/a = \langle\tfrac{1}{2}|J_z|\tfrac{1}{2}\rangle/\langle\tfrac{1}{2}|\tilde{S}_z|\tfrac{1}{2}\rangle\,. \quad (4.4)$$

The quadrupole term has no effect on an electronic doublet in a cubic environment but will not vanish in a Γ_8 quartet state. Spin-Hamiltonian parameters for the Kramers doublet systems studied are given in Table III.

At zero external field the spin Hamiltonian commutes with the effective total angular momentum operators

$$\vec{F} = \vec{\tilde{S}} + \vec{I}\,, \quad F_z = \tilde{S}_z + I_z\,, \quad (4.5)$$

and the energy eigenstates are of the form

$$\begin{aligned}|F, M_F\rangle = |I+\tfrac{1}{2}, M_F\rangle = &\left(\frac{I+M_F+\frac{1}{2}}{2I+1}\right)^{1/2}|\tilde{\tfrac{1}{2}}, M_F-\tfrac{1}{2}\rangle\\ &+\left(\frac{I-M_F+\frac{1}{2}}{2I+1}\right)^{1/2}|-\tilde{\tfrac{1}{2}}, M_F+\tfrac{1}{2}\rangle\,,\end{aligned}$$

with energy $E(I+\frac{1}{2}) = \frac{1}{2}AI$, and

$$\begin{aligned}|F-1, M_F\rangle = |I-\tfrac{1}{2}, M_F\rangle = &\left(\frac{I-M_F+\frac{1}{2}}{2I+1}\right)^{1/2}|\tilde{\tfrac{1}{2}}, M_F-\tfrac{1}{2}\rangle\\ &-\left(\frac{I+M_F+\frac{1}{2}}{2I+1}\right)^{1/2}|-\tilde{\tfrac{1}{2}}, M_F+\tfrac{1}{2}\rangle\,,\end{aligned}$$

with energy $E(I-\frac{1}{2}) = -\frac{1}{2}A(I+1)$. Kets on the right-hand side are in the form $|m_sm_I\rangle$. With a magnetic field imposed in the z direction the states become

$$\begin{aligned}|I+\tfrac{1}{2}, M_F\rangle_H &= a(H, M_F)|\tilde{\tfrac{1}{2}}, M_F-\tfrac{1}{2}\rangle + [1-a^2(H, M_F)]^{1/2}\\ &\quad\times|-\tilde{\tfrac{1}{2}}, M_F+\tfrac{1}{2}\rangle\,,\\ |I-\tfrac{1}{2}, M_F\rangle_H &= [1-a^2(H, M_F)]^{1/2}|\tilde{\tfrac{1}{2}}, M_F-\tfrac{1}{2}\rangle - a(H, M_F)\\ &\quad\times|-\tilde{\tfrac{1}{2}}, M_F+\tfrac{1}{2}\rangle\,,\end{aligned}$$

where

$$a(H, M_F) = \left(\frac{2\eta^2(M_F)}{\mu^2(H) + 4\eta^2(M_F) - \mu\,\mathrm{sgn}(A)[\mu^2(H) + 4\eta^2(M_F)]^{1/2}}\right)^{1/2},$$

TABLE III. Spin-Hamiltonian parameters, Eq. (4.3), for the Kramers-doublet systems $CaF_2:Tm^{2+}$ and $CaF_2:Ho^{2+}$. (See Sec. VI for $MgO:Er^{3+}$.)

Parameter	$CaF_2:{}^{169}Tm^{2+}$	$CaF_2:{}^{165}Ho^{2+}$
g	3.452	5.911
A (MHz)	−1101.4	−3921.3
g_n	0.756	48

TABLE IV. Crystal-field splitting and calculated wave functions for (a) Tm^{2+} ($4f^{13}\,{}^2F_{1/2}$) in CaF_2 (Ref. 25), (b) Ho^{2+} ($4f^{11}\,{}^4I_{15/2}$) in CaF_2 (Ref. 33), and Er^{3+} ($4f^{11}\,{}^4I_{15/2}$) in MgO (Ref. 10).

E (cm^{-1})	Wave functions
	(a)
588	$\lvert\Gamma_6 \pm \frac{1}{2}\rangle = \pm(\sqrt{7}/\sqrt{12})\lvert \pm \frac{1}{2}\rangle \pm (\sqrt{5}/\sqrt{12})\lvert \mp \frac{7}{2}\rangle$
	$\lvert\Gamma_8 \pm \frac{3}{2}\rangle = \frac{1}{2}\lvert \mp \frac{5}{2}\rangle + \frac{1}{2}\sqrt{3}\lvert \pm \frac{3}{2}\rangle$
555.8	$\lvert\Gamma_8 \pm \frac{1}{2}\rangle = (\sqrt{7}/\sqrt{12})\lvert \mp \frac{7}{2}\rangle - (\sqrt{5}/\sqrt{12})\lvert \pm \frac{1}{2}\rangle$
0	$\lvert\Gamma_7 \pm \frac{1}{2}\rangle = \pm\frac{1}{2}\sqrt{3}\lvert \pm \frac{5}{2}\rangle \mp \frac{1}{2}\lvert \mp \frac{9}{2}\rangle$
	(b)
	$\lvert\Gamma_8 \pm \frac{3}{2}\rangle = 0.4122\lvert \pm \frac{11}{2}\rangle + 0.7547\lvert \pm \frac{3}{2}\rangle + 0.3358\lvert \mp \frac{5}{2}\rangle + 0.3844\lvert \mp \frac{13}{2}\rangle$
33.5	$\lvert\Gamma_8 \pm \frac{1}{2}\rangle = -0.1836\lvert \pm \frac{9}{2}\rangle - 0.6389\lvert \pm \frac{1}{2}\rangle + 0.2631\lvert \mp \frac{7}{2}\rangle + 0.6992\lvert \mp \frac{15}{2}\rangle$
30.1	$\lvert\Gamma_7 \pm \frac{1}{2}\rangle = \pm(\sqrt{77}/8\sqrt{3})\lvert \pm \frac{13}{2}\rangle \pm (\sqrt{65}/8\sqrt{3})\lvert \pm \frac{5}{2}\rangle \mp \frac{1}{8}\sqrt{13}\lvert \mp \frac{9}{2}\rangle \mp (\sqrt{11}/8\sqrt{3})\lvert \mp \frac{11}{2}\rangle$
0	$\lvert\Gamma_6 \pm \frac{1}{2}\rangle = \pm(\sqrt{7}/8\sqrt{3})\lvert \pm \frac{9}{2}\rangle \pm \frac{1}{8}\sqrt{33}\lvert \pm \frac{1}{2}\rangle \pm \frac{1}{8}\sqrt{7}\lvert \mp \frac{7}{2}\rangle \pm (\sqrt{65}/8\sqrt{3})\lvert \mp \frac{15}{2}\rangle$
	(c)
	$\lvert\Gamma_8^{(2)} \pm \frac{3}{2}\rangle = 0.1644\lvert \pm \frac{11}{2}\rangle + 0.3995\lvert \pm \frac{3}{2}\rangle - 0.4643\lvert \mp \frac{5}{2}\rangle + 0.7731\lvert \mp \frac{13}{2}\rangle$
140	$\lvert\Gamma_8^{(2)} \pm \frac{1}{2}\rangle = -0.6084\lvert \pm \frac{9}{2}\rangle - 0.2400\lvert \pm \frac{1}{2}\rangle + 0.7534\lvert \mp \frac{7}{2}\rangle + 0.0677\lvert \mp \frac{15}{2}\rangle$
110	$\lvert\Gamma_7 \pm \frac{1}{2}\rangle = \pm(\sqrt{77}/8\sqrt{3})\lvert \pm \frac{13}{2}\rangle \pm (\sqrt{65}/8\sqrt{3})\lvert \pm \frac{5}{2}\rangle \mp \frac{1}{8}\sqrt{13}\lvert \mp \frac{9}{2}\rangle \mp (\sqrt{11}/8\sqrt{3})\lvert \mp \frac{11}{2}\rangle$
	$\lvert\Gamma_8^{(1)} \pm \frac{3}{2}\rangle = 0.9549\lvert \pm \frac{11}{2}\rangle - 0.2309\lvert \pm \frac{3}{2}\rangle + 0.1845\lvert \mp \frac{5}{2}\rangle + 0.0270\lvert \mp \frac{13}{2}\rangle$
0	$\lvert\Gamma_8^{(1)} \pm \frac{1}{2}\rangle = 0.7613\lvert \pm \frac{9}{2}\rangle - 0.4456\lvert \pm \frac{1}{2}\rangle + 0.4698\lvert \mp \frac{7}{2}\rangle + 0.0331\lvert \mp \frac{15}{2}\rangle$

$$\mu(H) = (g\mu_\beta - g_n\mu_N)H + AM_F ,$$

$$\eta(M_F) = \tfrac{1}{2}A[(I+M_F+\tfrac{1}{2})(I-M_F+\tfrac{1}{2})]^{1/2} ,$$

$$\mathrm{sgn}(A) = A/|A| ,$$

and the corresponding energies are

$$E(I\pm\tfrac{1}{2}, M_F) = -\tfrac{1}{4}A + g_n\mu_N HM_F \pm \mathrm{sgn}(A)\tfrac{1}{2}[A^2(I+\tfrac{1}{2})^2 + (g\mu_\beta - g_n\mu_N)^2H^2 + 2(g\mu_\beta - g_n\mu_N)HAM_F]^{1/2} .$$

We postpone discussion of the Zeeman and hyperfine interactions in the Γ_8 quartet, which are considerably more complicated than those in a doublet until Sec. IX, at which time MgO: Er^{3+} Γ_8 ground multiplet is considered in some detail.

V. DYNAMIC CRYSTAL-FIELD INTERACTION

In order to calculate spin-lattice relaxation rates for specific ions, an explicit form for the ion-lattice Hamiltonian (3.7) must be derived. It is necessary to choose a concrete model for this interaction and in what follows a point-charge crystal-field model is presumed valid. The method employed to obtain such an $\mathcal{H}_{il}$ is presented below in outline form. The derivation and results are basically equivalent to those of Buisson and Borg.[5] However, the present method employs vector and tensor methods to circumvent explicit evaluation of derivatives with respect to strain tensor components, resulting in a more straightforward approach.

The electrostatic potential energy of an electron belonging to a paramagnetic ion, whose instantaneous position is $\vec{R}_0$ (the electron is at $\vec{R}_0+\vec{r}$) is represented as

$$V(\vec{r}) = -\sum_{jl\,\Gamma a\beta} \frac{4\pi e Q_j r^l}{(2l+1)|\vec{R}_j - \vec{R}_0|^{l+1}} \times Y^*(l\,\Gamma a\beta;\theta_j\varphi_j)\,Y(l\,\Gamma a\beta;\theta\varphi) \quad . \qquad (5.1)$$

θ_j, φ_j are polar angles of the vector $\vec{R}_j - \vec{R}_0$. Expanding $V(\vec{r})$ about the lattice equilibrium configuration, in which the paramagnetic ion is at $\vec{R}_0^0 = \vec{0}$ and the jth point charge is at $\vec{R}_j^0$ yields

$$V(\vec{r}) = -\sum_{jl\,\Gamma a\beta} \frac{4\pi e Q_j r^l}{(2l+1)|R_j^0|^{l+1}} \times Y^*(l\,\Gamma a\beta;\theta_j^0\varphi_j^0)\,Y(l\,\Gamma a\beta;\theta\varphi) - \sum_{jl\,\Gamma a\beta} \frac{4\pi e Q_j}{2l+1}(\delta\vec{R}_j - \delta\vec{R}_0) \cdot \left(\vec{\nabla}_{(\vec{R}_j-\vec{R}_0)} \frac{Y^*(l\,\Gamma a\beta;\theta_j\varphi_j)}{|\vec{R}_j-\vec{R}_0|^{l+1}}\right)_{(\vec{R}_j^0-\vec{R}_0^0)} r^l Y(l\,\Gamma a\beta;\theta\varphi) + \cdots \quad . \qquad (5.2)$$

Here the first term is the usual static crystal-field interaction, while the remaining terms constitute the dynamic crystal-field interaction which is responsible for spin-lattice relaxation. In accord with the previous discussion we set $\mathcal{H}_{il}$ equal to the second term in (5.2), which in the long-wavelength

approximation (3.4), becomes

$$\mathcal{H}_{11} = -\sum_{j\, l\, \Gamma a\beta} \frac{4\pi e Q_j}{2l+1} \vec{R}_j^0 \cdot \vec{\sigma}(\vec{0}) \cdot \left(\vec{\nabla}_{(\vec{R}_j - \vec{R}_0)} \frac{Y^*(l\,\Gamma a\beta;\, \theta_j \varphi_j)}{|\vec{R}_j - \vec{R}_0|^{l+1}} \right)_{(\vec{R}_j^0 - \vec{R}_0^0)} \times r^l\, Y(l\,\Gamma a\beta;\, \theta\varphi) \,. \tag{5.3}$$

In order to separate the dynamic part of (5.3), i.e., $\vec{\sigma}(\vec{0})$, from the static terms the conjugate dyadic,

$$\overleftrightarrow{\sigma}^T = \sum_{i,j} \sigma_{ji} \hat{e}_i \hat{e}_j$$

is introduced so that the tensor identity

$$\vec{A} \cdot \overleftrightarrow{B} \cdot \vec{C} = \vec{A}\vec{C} : \overleftrightarrow{B}^T$$

may be employed, reducing (5.3) to the form

$$\mathcal{H}_{11} = -\sum_{j\, l\, \Gamma a\beta} \frac{4\pi e Q_j}{2l+1} \left[(\vec{R}_j - \vec{R}_0) \left(\vec{\nabla}_{(\vec{R}_j - \vec{R}_0)} \times \frac{Y^*(l\,\Gamma a\beta;\, \theta_j \varphi_j)}{|\vec{R}_j - \vec{R}_0|^{l+1}} \right) \right]_{(\vec{R}_j^0 - \vec{R}_0^0)} : \overleftrightarrow{\sigma}^T(\vec{0}) \times r^l\, Y(l\,\Gamma a\beta;\, \theta\varphi) \,, \tag{5.4}$$

where use has been made of the elementary properties of limits to simplify the term in square brackets.

Summation over ions can be decomposed into a summation over shells (s) of neighboring ions and a summation over ions (j') in each shell. Then, expanding the term in square brackets in terms of a complete set of cubic harmonics (functions of the *ion* coordinates), taking the limit $(\vec{R}_{j'} - \vec{R}_0) \to (\vec{R}_{j'}^0 - \vec{R}_0^0) = \vec{R}_{j'}^0$, Eq. (5.4) becomes

$$\mathcal{H}_{11}(\vec{r}) = -\sum_{\substack{sj'\, l\, \Gamma a\beta \\ l'\, \Gamma' a'\beta'}} \frac{4\pi e Q_s}{2l+1} c_{\Gamma'\beta'}\, Y(l'\,\Gamma' a'\beta';\, \theta_{j'}^0 \varphi_{j'}^0) \times \left\langle Y(l'\,\Gamma' a'\beta';\, \theta_{\vec{R}_{j'}^0} \varphi_{\vec{R}_{j'}^0}) \left| \vec{R}_{j'}^0 \vec{\nabla}_{\vec{R}_{j'}^0} \right| \times \frac{1}{|\vec{R}_{j'}^0|^{l+1}} Y^*(l\,\Gamma a\beta;\, \theta_{\vec{R}_{j'}^0} \varphi_{\vec{R}_{j'}^0}) \right\rangle : \overleftrightarrow{\sigma}^T(\vec{0}) r^l Y(l\,\Gamma a\beta;\, \theta\varphi) \,. \tag{5.5}$$

Since each shell of charges (in equilibrium configuation) transforms into itself under the operations of the cubic group, it follows that

$$\sum_{sj'} Q_s Y(l'\,\Gamma' a'\beta';\, \theta_{j'}^0 \varphi_{j'}^0) = \sum_s n_s Q_s Y(l'\,\Gamma_{1g};\, \theta_s \varphi_s) \delta(\Gamma', \Gamma_{1g}) \,,$$

in which n_s is the number of ions in shell s and R_s, θ_s, φ_s are the equilibrium coordinates of any one ion in that shell. A further simplification results if the dyadic operator

$$\overleftrightarrow{O} = \vec{R}_s \vec{\nabla}_{\vec{R}_s}$$

is employed. In terms of cubic components (3.6) the scalar product $\overleftrightarrow{O} : \overleftrightarrow{\sigma}^T$ is then

$$\overleftrightarrow{O} : \overleftrightarrow{\sigma}^T = \sum_{\Gamma\beta} c_{\Gamma\beta} O(\Gamma\beta) \sigma^T(\Gamma\bar{\beta}) = \sum_{\Gamma\beta} c_{\Gamma\beta} c'_\Gamma O(\Gamma\beta) \sigma(\Gamma\bar{\beta}) \,.$$

It is easy to show that

$$c'_{\Gamma_4} = -1$$

and

$$c'_{\Gamma_{1g}} = c'_{\Gamma_{3g}} = c'_{\Gamma_{5g}} = 1 \,.$$

Finally, making use of the further simplification that

$$\left\langle Y(l'\,\Gamma_{1g}) \left| O(\Gamma'\beta') \right| \frac{1}{R_s^{l+1}} Y^*(l\,\Gamma a\beta) \right\rangle$$

vanishes unless $\Gamma' = \Gamma$ and $\beta' = \beta$, the first-order ion-lattice interaction potential at a cubic site becomes

$$\mathcal{H}_{11} = -\sum_{\substack{s\, l\, \Gamma a\beta \\ l'}} \frac{4\pi e n_s Q_s}{2l+1} c_{\Gamma\beta} c'_\Gamma Y(l'\,\Gamma_{1g};\, \theta_s \varphi_s) \times \left\langle Y(l'\,\Gamma_{1g}) \left| O(\Gamma\beta) \right| \frac{1}{R_s^{l+1}} Y^*(l\,\Gamma a\beta) \right\rangle \times \sigma_0(\Gamma\bar{\beta}) r^l Y(l\,\Gamma a\beta;\, \theta\varphi) \,. \tag{5.6}$$

The total ion-lattice interaction is thus of the form

$$\mathcal{H}_{11} = \sum_{l\, \Gamma a\beta} V'(l\,\Gamma a\beta)\, c_{\Gamma\beta}\, Y(l\,\Gamma a\beta;\, \theta\varphi) \sigma_0(\Gamma\bar{\beta}) \tag{5.7}$$

and the coefficients, which are independent of the index β, are given by

$$V'(l\,\Gamma a\beta) = -\sum_{sl'} \frac{4\pi e n_s Q_s}{2l+1} c'_\Gamma Y(l'\,\Gamma_{1g};\, \theta_s \varphi_s) r^l \times \left\langle Y(l'\,\Gamma_{1g}) \left| O(\Gamma\beta) \right| \frac{1}{R_s^{l+1}} Y^*(l\,\Gamma a\beta) \right\rangle \,. \tag{5.8}$$

The matrix element is easily evaluated:

$$\left\langle Y(l'\,\Gamma_{1g}) \left| O(\Gamma\beta) \right| \frac{1}{R_s^{l+1}} Y^*(l\,\Gamma a\beta) \right\rangle = \sum_{\substack{m_1 m_2 \\ m_3 l'' \\ m'' q}} \langle l' m_1 | l'\,\Gamma_{1g} \rangle \langle n m_2 | n\,\Gamma\beta \rangle \langle l - m_3 | l\,\Gamma a\beta \rangle \times \frac{(-1)^{l''-m''+l}}{3} \langle l'\, m_1\, l''\, -m'' | l'\, l''\, 1\, q \rangle \times \langle l'' m'' l - m_3 | l'' l 1 m_2 - q \rangle \langle 1\, q\, 1\, m_2 - q | 1\, 1\, n\, m \rangle \times \langle Y_{l'} \| R_s \| Y_{l''} \rangle \langle Y_{l''} \| \nabla \| (1/R_s^{l+1}) Y_l \rangle \,. \tag{5.9}$$

The first three symbols on the right-hand side of Eq. (5.9) are the transformation coefficient from spherical harmonics to "cubic" harmonics.[19] The parameter n appearing in the second symbol is 0 for $\Gamma = \Gamma_{1g}$, 1 for $\Gamma = \Gamma_{4g}$, and 2 for $\Gamma = \Gamma_{3g}$ or Γ_{5g}. The following three symbols are Clebsch-Gordan coefficients. The only nonzero reduced matrix elements of concern are

TABLE V. Dynamic crystal-field parameters $V(l\Gamma a)$ [Eq. (5.11)] for $CaF_2:Tm^{2+}$, $CaF_2:Ho^{2+}$, $MgO:Er^{3+}$. $V(2\Gamma)$ converges rather slowly as additional shells of neighboring ions are considered. All ions within 12-nearest-neighbor distances of the paramagnetic ion site have been included.

	$CaF_2:Tm^{2+}$ cm^{-1}	$CaF_2:Ho^{2+}$ cm^{-1}	$MgO:Er^{3+}$ cm^{-1}
$V(2\Gamma_{3g})$	8922	9346	−34100
$V(2\Gamma_{5g})$	−5948	−6231	22730
$V(4\Gamma_{1g})$	−5633	−8784	13660
$V(4\Gamma_{3g})$	4281	6676	10600
$V(4\Gamma_{4g})$	3563	5555	−8640
$V(4\Gamma_{5g})$	−8851	−13800	−6519
$V(6\Gamma_{1g})$	4947	5309	4071
$V(6\Gamma_{3g})$	−1532	−1644	−5339
$V(6\Gamma_{4g})$	3238	3475	2665
$V(6\Gamma_{5g}a)$	1478	1586	1216
$V(6\Gamma_{5g}b)$	368	395	3581

$$\langle Y_{l+1}\|\nabla\|(1/R_s^{l+1})Y_l\rangle = -(2l+1)(l+1)^{1/2}\frac{1}{R_s^{l+2}},$$
$$\langle Y_{l+2}\|R_s\|Y_{l+1}\rangle = (l+2)^{1/2}R_s, \qquad (5.10)$$
$$\langle Y_l\|R_s\|Y_{l+1}\rangle = -(l+1)^{1/2}R_s.$$

In conformity with convention and for ease of computation $\mathcal{H}_{11}$ is expressed

$$\mathcal{H}_{11} = \sum_{l\Gamma a\beta} V(l\Gamma a)C(l\Gamma a\beta;\theta\varphi)\sigma_0(\Gamma\bar{\beta}), \qquad (5.11)$$

using Racah's spherical harmonics

$$C(l\Gamma a\beta;\theta\varphi) = [4\pi/(2l+1)]Y(l\Gamma a\beta;\theta\varphi).$$

The ion-lattice coefficients $V(l\Gamma a)$ for the systems studied are presented in Table V.

VI. SPIN-LATTICE RELAXATION IN SPECIFIC SYSTEMS

It is probably appropriate to emphasize at this point that we are working with a well-defined simple model, and calculations are primarily a test of the utility of that model. A minimum of experimental parameters are used; only those necessary to differentiate one system from another. The calculations employ experimental values of $\langle r^4\rangle$ and $\langle r^6\rangle$ so as to maintain consistency in static and dynamic crystal fields, and a computed[24] value of $\langle r^2\rangle$, since this parameter is not obtainable from experiment for systems under consideration. The lattice dynamics (phonon modes, density of states, etc.) are entirely characterized in the present model by the velocities of sound v_L and v_T.

A. $CaF_2:Tm^{2+}$

While the properties of divalent thulium in a cubic environment have been studied by many investigators, understanding of this relatively simple system is far from complete. The optical spectrum of $CaF_2:Tm^{2+}$ ($4f^{13}-{}^2F_{7/2}$ free-ion ground term) was observed by Kiss[25] who found that a Γ_7 doublet lies lowest with a Γ_8 quartet at 555.8 cm^{-1}. Based on Kiss's data and a point-charge model, Bleaney[26] obtained effective values of $\langle r^4\rangle$ and $\langle r^6\rangle$ considerably larger than those calculated by Freeman and Watson[24] and predicted that the Γ_6 doublet would lie at 588 cm^{-1}. High-precision spin-Hamiltonian parameters have been provided by the electron-nuclear-double-resonance (ENDOR) experiments of Bessent and Hayes.[27]

The system is characterized by a spin Hamiltonian (4.3) with $\tilde{S}=\frac{1}{2}$, $I=\frac{1}{2}$. At zero magnetic field, eigenstates for $CaF_2:Tm^{2+}$ are then a triply degenerate lower hyperfine level

$$|1\,1\rangle = \left|\tfrac{\tilde{1}}{2}\,\tfrac{1}{2}\right\rangle,$$
$$|1\,0\rangle = (1/\sqrt{2})\left|\tfrac{\tilde{1}}{2}-\tfrac{1}{2}\right\rangle + (1/\sqrt{2})\left|-\tfrac{\tilde{1}}{2}\,\tfrac{1}{2}\right\rangle, \qquad (6.1)$$
$$|1-1\rangle = \left|-\tfrac{\tilde{1}}{2}-\tfrac{1}{2}\right\rangle,$$

transforming as Γ_5 in the cubic group and an excited hyperfine singlet

$$|0\,0\rangle = (1/\sqrt{2})\left|\tfrac{\tilde{1}}{2}-\tfrac{1}{2}\right\rangle - (1/\sqrt{2})\left|-\tfrac{\tilde{1}}{2}\,\tfrac{1}{2}\right\rangle \qquad (6.2)$$

at 1104.1 MHz, transforming as Γ_2. The $|1\,1\rangle$ and $|1-1\rangle$ states remain eigenstates at arbitrary field while the remaining states correlate to

$$|1\,0\rangle_H = -(A/2g\mu_\beta H)\left|\tfrac{\tilde{1}}{2}-\tfrac{1}{2}\right\rangle + \left|-\tfrac{\tilde{1}}{2}\,\tfrac{1}{2}\right\rangle,$$
$$|0\,0\rangle_H = \left|\tfrac{\tilde{1}}{2}-\tfrac{1}{2}\right\rangle + \frac{A}{2g\mu_\beta H}\left|-\tfrac{\tilde{1}}{2}\,\tfrac{1}{2}\right\rangle. \qquad (6.3)$$

Hyperfine levels at high field are given schematically in Fig. 1.

1. Direct process

Considering first the direct-process equation (3.32)

$$\langle j\,|\,V(\Gamma\beta)\,|\,i\rangle = 0$$

as expected,[9] when $|j\rangle$ and $|i\rangle$ are zeroth-order hyperfine states and $V(\Gamma\beta)$ acts only on the electron coordinates. However, Zeeman and hyperfine interactions do admix hyperfine levels derived from excited electronic states into the ground multiplet. Since it is a consequence of group theory that $\vec{J}$ does not connect Γ_7 and Γ_6 states, perturbed hyperfine levels are of the form

$$|FM_F\rangle'_H = |FM_F\rangle_H - \sum_{m_S=-3/2}^{3/2}\sum_{m_I} \times \frac{|\Gamma_8 m_S m_I\rangle\langle\Gamma_8 m_S m_I|\mathcal{H}_J|FM_F\rangle_H}{E(\Gamma_8)}, \qquad (6.4)$$

where $\mathcal{H}_J$ is given by Eq. (4.2). With hyperfine states in this form, Eq. (3.32) yields a nonvanish-

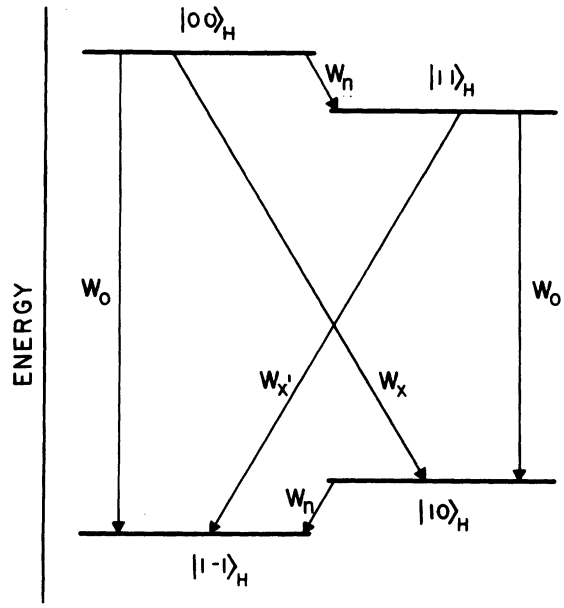

FIG. 1. Schematic representation of hyperfine levels of $^{169}Tm^{2+}$ in CaF_2 at high magnetic field. Downward transition rates W_0, W_x, $W_{x'}$, W_n refer to allowed, $\Delta M_F = 0$ "skew," $\Delta M_F = 2$ "skew," and nuclear transitions, respectively. See Eq. (6.17) and discussion.

ing direct process transition rate. T^{ij} has been calculated for all possible transitions in this system with an external magnetic field ranging from 0 to 10^5 G parallel to the crystal [100] axis. The experimental sound velocities $v_L = 7.36\times10^5$, $v_T = 3.34\times10^5$ cm/sec of the pure CaF_2 lattice were employed.[28]

At zero external field a state-to-state direction corrected direct process rate

$$T^{ij} = 5.68\times10^{-7}T\ (\mathrm{sec}^{-1})$$

is obtained for transitions between $|i\rangle = |00\rangle$ and any one of the degenerate states $|j\rangle = |1M_F\rangle$. It is a direct consequence of the cubic group symmetries of the zero-field states (Γ_2, Γ_5) that only the Γ_{4g} lattice modes are involved in the direct process at zero field. The role of these "rotational" lattice modes in spin lattice relaxation has until recently[11] been neglected by almost all authors. The kinetic equation (3.24) for the behavior of the population of $|00\rangle P_0$ and the population of the triply degenerate level $|1M_F\rangle P_1$ is thus

$$\frac{d}{dt}\begin{bmatrix}P_0\\P_1\end{bmatrix} = \begin{bmatrix}-3T^{ij}\,e^{\delta/2kT} & T^{ij}\,e^{-\delta/2kT}\\ 3T^{ij}\,e^{\delta/2kT} & -T^{ij}\,e^{-\delta/2kT}\end{bmatrix}\begin{bmatrix}P_0\\P_1\end{bmatrix}, \tag{6.5}$$

$$\delta = E_{|00\rangle} - E_{|11\rangle}\,.$$

The corresponding reduced transition-rate matrix

$$\tilde{W}^{\mathrm{lev}} = \begin{bmatrix}-3T^{ij}\,e^{\delta/2kT} & \sqrt{3}T^{ij}\\ \sqrt{3}T^{ij} & -T^{ij}\,e^{-\delta/2kT}\end{bmatrix} \tag{6.6}$$

has a single nonzero eigenvalue $\lambda = T^{ij}(e^{-\delta/2kT} + 3e^{\delta/2kT})$. The return of this system to thermal equilibrium is characterized by an approximate zero-field relaxation inverse time or rate

$$1/T_1 \approx 2.27\times10^{-6}T\ (\mathrm{sec}^{-1})\ . \tag{6.7}$$

Results at nonzero external field are expressed in terms of the direction corrected relaxation rate between nondegenerate levels

$$T^{ij}_{\mathrm{direct}} = (t_3^{ij} + t_4^{ij} + t_5^{ij})\,T\ , \tag{6.8}$$

in which t_n^{ij} is the contribution of the Γ_{ng} lattice modes to the relaxation.

A convenient classification of relaxation rates at high field is indicated in Fig. 1. In the high-field limit the allowed EPR transitions $|\Delta M_F| = 1$ between $|11\rangle$ and $|10\rangle$ and between $|00\rangle$ and $|1-1\rangle$ have a total symmetrized direct process transition rate (related to W_0 in Fig. 1)

$$T^{ij}_{\mathrm{direct}} = \frac{1}{12\pi\rho\hbar}\left(\frac{g\mu_B H}{\hbar}\right)^3 \mathrm{cosech}\left(\frac{g\mu_B H}{2kT}\right) \times \sum_{X\Gamma}\frac{C(X,\Gamma)}{v_X^5}\,\frac{4\,|\langle\tfrac{1}{2}|\,g_J\mu_B H J_g\,|\,\Gamma_8-\tfrac{3}{2}\rangle|^2}{[E(\Gamma_8)]^2} \times \sum_{\beta}|\langle\Gamma_8-\tfrac{3}{2}|\,V(\Gamma\beta)\,|-\tfrac{1}{2}\rangle|^2\ . \tag{6.9}$$

Since ion-lattice relaxation within either pair of these levels ($|11\rangle \rightleftharpoons |10\rangle$ and $|00\rangle \rightleftharpoons |1-1\rangle$, see Fig. 1) occurs much faster than lattice-induced transitions from either member of the pair to any other level, return of the populations of these levels to thermal equilibrium after a short saturating pulse will be characterized by a single exponential decay (relaxation time)

$$1/T_1 = 5.6\times10^{-15}H^4T\ \ (kT \ll g\mu_B H)\ . \tag{6.10}$$

EPR "skew" transitions with $|\Delta M_F| = 2$ between $|11\rangle$ and $|1-1\rangle$ and with $|\Delta M_F| = 0$ between $|00\rangle$ and $|10\rangle$ involve essentially a nuclear spin flip, so that ion-lattice transition rates are smaller, owing to the fact that $\mathcal{H}_{11}$ does not affect the nuclear states. In the high-field limit these transition rates increase as H^2T. Return of a population disturbance to thermal equilibrium will generally occur in a multiexponential manner.

Nuclear transitions rates between $|00\rangle$ and $|11\rangle$ and between $|10\rangle$ and $|1-1\rangle$ are very small and actually decrease with increasing field.

We present some calculated values for the t_n^{ij}, direct process Eq. (6.8), at intermediate fields in Table VI. No transition is connected with all three sets of lattice modes. The two allowed EPR transitions are coupled to Γ_{4g} and Γ_{5g} modes, $|\Delta M_F| = 2$ skew transitions involve Γ_{3g} and Γ_{5g} modes, the

TABLE VI. Contributions t_n^{ij} ($\sec^{-1}K^{-1}$) of the Γ_{ng} lattice modes to the direct relaxation process for $CaF_2:Tm^{2+}$. The direction-corrected relaxation rate is given by $T_{\text{direct}}^{ij}=(t_3^{ij}+t_4^{ij}+t_5^{ij})T$. At $H=0$; $t_3^{|00\rangle,|1m\rangle}=t_5^{|00\rangle,|1m\rangle}=0$, $t_4^{|00\rangle,|1m\rangle}=5.68\times10^{-7}$ $\sec^{-1}K^{-1}$.

		$H=100$ G			$H=10^4$ G		
i	j	t_3^{ij}	t_4^{ij}	t_5^{ij}	t_3^{ij}	t_4^{ij}	t_5^{ij}
$\|11\rangle$	$\|10\rangle$	0	3.94×10^{-9}	4.41×10^{-8}	0	4.03	21.0
$\|11\rangle$	$\|1-1\rangle$	1.09×10^{-7}	0	5.71×10^{-7}	1.09×10^{-3}	0	5.71×10^{-3}
$\|11\rangle$	$\|00\rangle$	0	1.58×10^{-7}	6.02×10^{-7}	0	8×10^{-12}	1.53×10^{-6}
$\|10\rangle$	$\|1-1\rangle$	0	3.11×10^{-10}	1.55×10^{-7}	0	1×10^{-11}	1.44×10^{-6}
$\|10\rangle$	$\|00\rangle$	3.27×10^{-7}	6.78×10^{-7}	0	3.27×10^{-3}	1.10×10^{-3}	0
$\|1-1\rangle$	$\|00\rangle$	0	2.04×10^{-6}	2.49×10^{-6}	0	4.41	23.0

$\Delta M_F=0$ transition involves Γ_{3g} and Γ_{4g} modes, and high-field "nuclear" transitions involve Γ_{4g} and Γ_{5g} modes.

2. *Raman process*

The only other relaxation mechanism available to the system under consideration is the Raman process. While it is certain that matrix elements of the effective perturbation (3.34) between the ion states $|\tilde{\tfrac{1}{2}}\pm\tfrac{1}{2}\rangle$ and $|-\tilde{\tfrac{1}{2}}\pm\tfrac{1}{2}\rangle$ will exhibit the "Van Vleck" cancellation (3.42a), it is not readily apparent whether (3.42a) will hold for all pairs of initial and final states at arbitrary field since electronic matrix elements which occur in the calculation are of the form

$$\langle\pm\tfrac{1}{2}|\,V(\Gamma_1\beta_1)\,|t\rangle\langle t|\,V(\Gamma_2\beta_2)\,|\pm\tfrac{1}{2}\rangle\quad,$$

as well as the usual

$$\langle\pm\tfrac{1}{2}|\,V(\Gamma_1\beta_1)\,|t\rangle\langle t|\,V(\Gamma_2\beta_2)\,|\mp\tfrac{1}{2}\rangle\quad.$$

It can be demonstrated however, that Eq. (3.42) does, in general, apply to these calculations[29,30] owing to the following identities, resulting from time reversal symmetry:

$$\langle\tfrac{1}{2}|\,V_1\,|\tfrac{1}{2}'\rangle\langle\tfrac{1}{2}'|\,V_2\,|-\tfrac{1}{2}\rangle = -\langle\tfrac{1}{2}|\,V_2\,|-\tfrac{1}{2}'\rangle\langle-\tfrac{1}{2}'|\,V_1\,|-\tfrac{1}{2}\rangle\quad,$$

$$\langle\tfrac{1}{2}|\,V_1\,|\tfrac{1}{2}'\rangle\langle\tfrac{1}{2}'|\,V_2\,|\tfrac{1}{2}\rangle = \langle-\tfrac{1}{2}|\,V_2\,|-\tfrac{1}{2}'\rangle\langle-\tfrac{1}{2}'|\,V_1\,|-\tfrac{1}{2}\rangle\quad,$$

in which $|\pm\tfrac{1}{2}\rangle$ and $|\pm\tfrac{1}{2}'\rangle$ are pairs of Kramers conjugate states and V_1, V_2 are time-even operators. Thus Raman relaxation in this system displays a characteristic T^9 dependence.

We have calculated the Raman relaxation rate for all transitions from zero to high magnetic fields. The zero-field transition $|00\rangle\rightarrow|1M_F\rangle$,

$$T^{00,1M_F}=1.93\times10^{-7}T^9\ (\sec^{-1}) \qquad (6.11a)$$

and

$$\tilde{W}_{01}^{\text{lev}}=3.34\times10^{-7}T^9\ (\sec^{-1})\quad, \qquad (6.11b)$$

corresponding to a level-to-level relaxation time given by $1/T_1=7.7\times10^{-7}T^9$ ($\sec^{-1}$) so that Raman-process relaxation becomes comparable with the direct process below 2 K. In general, all lattice vibrational modes are involved in Raman relaxation. Some calculated Raman reduced transition rates for nonzero magnetic field can be found in Table VII. Change in Raman transition rates with increasing field arise essentially from changes in wavefunctions. At high fields relaxation rates for allowed EPR transitions become field independent and a relaxation rate

$$1/T_1=8.2\times10^{-7}T^9\ (\sec^{-1}) \qquad (6.12)$$

for the Raman process is obtained. For skew and nuclear transitions, relaxation rates exhibit a $H^{-2}T^9$ dependence at large field.

3. *Summary of calculations and comparison with experiment*

The calculated relaxation behavior at zero field is described by the relaxation rate

$$1/T_1=(2.27\times10^{-6}T+7.7\times10^{-7}T^9)\ (\sec^{-1})\quad. \qquad (6.13)$$

In the high-field limit relaxation of the allowed EPR transitions is also governed by a relaxation rate

$$1/T_1=(5.6\times10^{-15}H^4T+8.2\times10^{-7}T^9)\ (\sec^{-1})\,. \qquad (6.14)$$

TABLE VII. Direction-corrected relaxation rates T^{ij} for the Raman relaxation process in $CaF_2:Tm^{2+}$. See Eq. (3.44). Entries are normalized with respect to T^9. At $H=0$ $T^{|00\rangle-|11\rangle}=T^{|00\rangle-|10\rangle}=T^{|00\rangle-|1-1\rangle}=1.93\times10^{-7}T^9$ $\sec^{-1}$.

		T^{ij}/T^9 ($\sec^{-1}K^9$)	T^{ij}/T^9 ($\sec^{-1}K^{-9}$)
i	j	$H=100$ G	$H=10^4$ G
$\|11\rangle$	$\|10\rangle$	2.70×10^{-7}	3.86×10^{-7}
$\|11\rangle$	$\|1-1\rangle$	0	0
$\|11\rangle$	$\|00\rangle$	1.15×10^{-7}	5.00×10^{-11}
$\|10\rangle$	$\|1-1\rangle$	1.15×10^{-7}	5.00×10^{-11}
$\|10\rangle$	$\|00\rangle$	1.62×10^{-7}	1.00×10^{-10}
$\|1-1\rangle$	$\|00\rangle$	2.70×10^{-7}	3.86×10^{-7}

where H is in gauss and T in kelvin. Relaxation at low field exhibits a multiexponential return to equilibrium.

Huang[6] made the first measurement of spin-lattice relaxation in this system, finding for the allowed EPR transitions with $H=2$ kG along the crystal [100] axis, a relaxation rate for 0.2-mole% Tm^{2+} in CaF_2,

$$1/T_1 = (13T + 7.7\times10^{-8}T^9)\ (\text{sec}^{-1}) \quad . \qquad (6.15)$$

In a subsequent study by Sabisky and Anderson[31] the magnetic field was varied over the range 1–12 kG. It was found that the direct process included an anomalous component which was approximately field independent. The true direct process, proportional to H^4T, was identified and was found to contribute

$$1/T_1 = 5.9\times10^{-16}H^4T \quad (H \text{ in G and } T \text{ in K}) \qquad (6.16)$$

to the relaxation. In addition a Raman process, in agreement with Huang, was found. Comparing calculated results with experiment, the direct-process result (6.10) and Raman process result (6.13) are a factor of 10 larger than experiment [Eq. (6.16)]. We feel these results to be reasonably satisfactory considering the simplicity of the model employed.

Recently, this system together with $SrF_2:Tm^{2+}$ was studied by Abragam *et al.*[11] at $H\approx 27$ kG and very low temperature ($T\sim 0.6$ K). Downward transition rates (W_0, W_x, W_x' in Fig. 1) at such low temperatures ($kT \ll \hbar\omega$) are almost entirely due to spontaneous emission of phonons and are therefore nearly temperature independent. Contributions B_3, B_4, B_5 of the Γ_{3g}, Γ_{4g}, Γ_{5g} lattice modes may be related to the spontaneous transition rates by[11]

$$\begin{aligned} W_0 &= \tfrac{1}{2}(B_4 + B_5) = W_{|00\rangle\to|1\text{-}1\rangle} = W_{|11\rangle\to|10\rangle} \quad , \\ W_x &= \left(\frac{A}{2g\mu_B H}\right)^2 (9B_3 + B_4) = W_{|00\rangle\to|10\rangle} \quad , \qquad (6.17) \\ W_{x'} &= \left(\frac{A}{2g\mu_B H}\right)^2 (3B_3 + B_5) = W_{|11\rangle\to|1\text{-}1\rangle} \quad , \end{aligned}$$

when $\vec{H}$ is parallel to the [100] axis. The experimental values for B_3, B_4, and B_5 together with calculated values are presented in Table VIII. While there is clearly quite good agreement for B_3 and B_4 in both systems, calculated values of B_5 are much greater than experimental ones. One is struck as well by the difference in measured B_5 values for CaF_2 and SrF_2. Calculated values of B_3, B_4, and B_5 prove quite sensitive to small variations in the parameter $\langle r^2\rangle$, somewhat less sensitive to changes in $\langle r^4\rangle$, and quite insensitive to changes in $\langle r^6\rangle$. A 10% increase or decrease of $\langle r^2\rangle$ from the Hartree-Fock value induced over 25% increase or decrease in the calculated B_5. An attempt to fit the three experimentally determined quantities in both CaF_2 and SrF_2 hosts to any set of $\langle r^2\rangle$, $\langle r^4\rangle$, $\langle r^6\rangle$ has been unsuccessful, although a far better estimate of the total relaxation magnitude obtains with $\langle r^2\rangle$ at about one-half the Hartree-Fock value, indicating perhaps a significant diamagnetic shielding contribution.[10,32] We hope that planned investigations of these systems incorporating covalent effects and a realistic lattice spectrum (including effects of the impurity perturbation) will yield an explanation for the unusual character of the Γ_{5g} contribution.

B. $CaF_2:Ho^{2+}$

The optical spectrum of $CaF_2:Ho^{2+}$ ($4f^{11}$, $^4I_{15/2}$ ground free-ion state), first observed by Weakleim and Kiss,[33] indicates that this system possesses a lowest Γ_6 doublet, with a low-lying Γ_7 doublet at 30.1 cm^{-1} and a Γ_8 quartet at 33.5 cm^{-1}. Spin-Hamiltonian parameters are provided by the paramagnetic resonance experiments of Lewis and Sabisky.[34] The system is characterized by the spin Hamiltonian (4.3) with $\tilde{S}=\frac{1}{2}$, $I=\frac{7}{2}$. Most notable for this system is the large value of the magnetic hyperfine parameter $A=-0.1307$ cm^{-1}, implying significant mixing of electronic states by the hyperfine interaction even at moderately high fields (<10 kG).

Diagonalizing the spin Hamiltonian (4.3) for $CaF_2:Ho^{2+}$ at zero field yields a ninefold degenerate lower hyperfine level

$$\begin{aligned} |\,4, M_F\rangle = &[\tfrac{1}{8}(4+M_F)]^{1/2}\,|\,\tfrac{1}{2}, M_F - \tfrac{1}{2}\rangle \\ &+ [\tfrac{1}{8}(4-M_F)]^{1/2}\,|\,-\tfrac{1}{2}, M_F + \tfrac{1}{2}\rangle , \qquad (6.18) \end{aligned}$$

whose component states transform in the cubic group O as $\Gamma_1+\Gamma_3+\Gamma_4+\Gamma_5$ and a sevenfold degenerate excited hyperfine level

$$\begin{aligned} |\,3, M_F\rangle = &[\tfrac{1}{8}(4-M_F)]^{1/2}\,|\,\tfrac{1}{2}, M_F - \tfrac{1}{2}\rangle \\ &- [\tfrac{1}{8}(4+M_F)]^{1/2}\,|\,-\tfrac{1}{2}, M_F + \tfrac{1}{2}\rangle \qquad (6.19) \end{aligned}$$

at 15.67 GHz whose component states transform as $\Gamma_2+\Gamma_4+\Gamma_5$. The ninefold and sevenfold degeneracies are, however, an artifact of the spin-Hamiltonian formalism. Diagonalizing the Hamiltonian

$$\mathcal{H}_j(H=0) = a\vec{I}\cdot\vec{J} \qquad (6.20)$$

TABLE VIII. Contributions of the Γ_{3g}, Γ_{4g}, Γ_{5g} lattice modes to direct-process relaxation in the low-temperature high-field (~27 kG) region for $CaF_2:Tm^{2+}$ and $SrF_2:Tm^{2+}$. See Eq. (6.17).

	$CaF_2:Tm^{2+}$		$SrF_2:Tm^{2+}$	
	Expt.	Calc.	Expt.	Calc.
B_3 (sec^{-1})	800	870	1800	1700
B_4 (sec^{-1})	2300	2740	2000	3700
B_5 (sec^{-1})	<100	14300	6500	26900

for the entire $J=\frac{15}{2}$, $I=\frac{7}{2}$ manifold removes the degeneracies among the cubic components of the $F=4$ level (total splitting ≈ 2.1 MHz) and the $F=3$ level (total splitting ≈ 0.7 MHz). Experiment will reveal under which conditions (if any) these small splittings are observable. For the present study we assume that hyperfine linewidths are sufficiently broad that the $F=4$ and $F=3$ levels may be treated as degenerate. Comparison of the eigenstates of (6.20) with the zeroth- and first-order eigenstates employed in the relaxation-rate calculations implies less than a 10% difference in calculated rates between the exact (6.20) and perturbation treatments. Hyperfine levels at zero field and at $H=2.4$ kG are given in Fig. 2.

1. Direct process

Direct-process relaxation in this system is subject to the same general considerations as for $CaF_2:Tm^{2+}$. The direct process is permitted only by Zeeman or hyperfine admixture of the Γ_8 excited electronic states. Since the excited Γ_8 state lies at 33.8 cm^{-1}, direct-process relaxation in $CaF_2:Ho^{2+}$ is much larger than for $CaF_2:Tm^{2+}$.

Direct-process relaxation at zero field is characterized by the level-to-level reduced transition rate

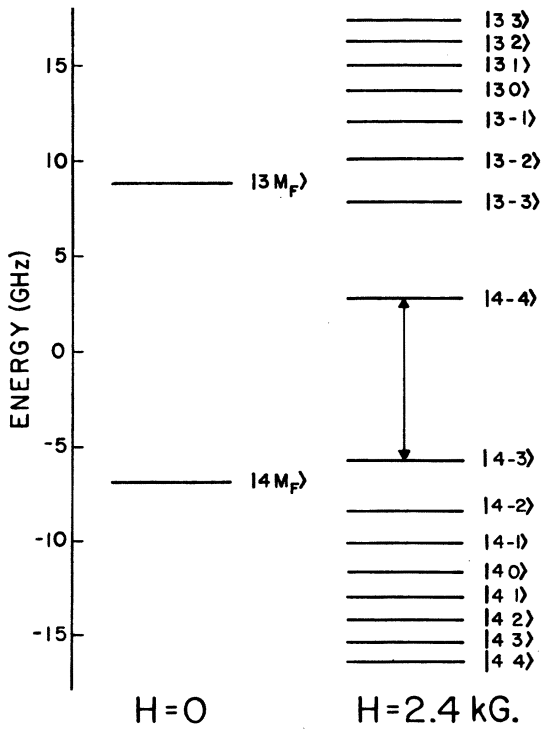

FIG. 2. Hyperfine energy levels of $^{165}Ho^{2+}$ in CaF_2 at zero field and at $H=2.4$ kG. The transition indicated at high field is that studied by Huang (Ref. 6).

$$\tilde{W}_{kl}^{1ev}=14.7T\ \text{sec}^{-1}\ , \tag{6.21}$$

where k and l refer to the levels composed of $|4M_F\rangle$ states and of $|3M_F\rangle$ states, respectively. Diagonalizing $\tilde{W}^{1ev}$ yields a relaxation rate for the two-level zero-field system of

$$1/T_1=33.2T\ \text{sec}^{-1}\ . \tag{6.22}$$

Direct-process relaxation in $CaF_2:Ho^{2+}$ at zero field is thus expected to occur some 10^7 times faster than in $CaF_2:Tm^{2+}$. This large difference in relaxation rate is attributed to (i) the low-lying excited Γ_8 electronic level and (ii) the large hyperfine-coupling constant in the $CaF_2:Ho^{2+}$ system.

Results at a moderate value of external magnetic field (2.4 kG) are given in Table IX, expressed in terms of the contribution of the Γ_{3g}, Γ_{4g}, and Γ_{5g} lattice modes to the direction corrected relaxation rate [Eq. (6.8)]. The largest transition rates are associated with allowed EPR transitions and attributed to Γ_{4g} and Γ_{5g} modes. Relatively large skew transition rates are attributed to the large magnetic hyperfine interaction in this system.

2. Raman processes

Raman-process relaxation at zero field is characterized by the level-to-level reduced transition rate

$$\tilde{W}_{kl}^{1ev}=2.18\times10^{-4}T^9\ \text{sec}^{-1} \tag{6.23}$$

and a corresponding relaxation time is given by

$$1/T_1=4.19\times10^{-4}T^9\ \text{sec}^{-1}\ . \tag{6.24}$$

Owing to the large magnetic hyperfine-constant Raman rates for the various allowed EPR transitions are different in the usual "high-field" region. Raman rates at a 2.4-kG external magnetic field are included in Table IX. Raman relaxation is clearly largest for the allowed EPR transitions.

In $CaF_2:Ho^{2+}$, resonant Raman relaxation may occur via either the Γ_7 electronic level at 30.1 cm^{-1} and the Γ_8 level at 33.5 cm^{-1}. Resonant Raman relaxation at zero field is characterized by

$$\tilde{W}_{kl}^{1ev}=1.05\times10^9\,e^{-43.3/T}+6.77\times10^9\,e^{-48.2/T}, \tag{6.25}$$

$$1/T_1=2.11\times10^9\,e^{-43.3/T}+1.36\times10^{10}\,e^{-48.2/T}. \tag{6.26}$$

Resonant Raman rates at 2.4 kG are also included in Table IX and are seen to be greatest for the allowed EPR transitions.

3. Summary and comparison with experiment

Relaxation behavior of $CaF_2:Ho^{2+}$ at zero field is described by a total inverse relaxation time

$$1/T_1=33.2T+4.19\times10^4T^9+2.11\times10^9\,e^{-43.3/T}+1.36\times10^{10}\,e^{-48.2/T}\ . \tag{6.27}$$

TABLE IX. Relaxation processes in $CaF_2:Ho^{2+}$ at $H=2.4$ kG along a crystal [100] axis. The direct-process direction-corrected relaxation rate is given by $T_{\text{direct}}^{ij}=(t_3^{ij}+t_4^{ij}+t_5^{ij})T$. Raman rates are normalized with respect to T^9 while resonance Raman rates are normalized with respect to $e^{-\Delta/kT}$. Only the larger relaxation rates, corresponding in general to allowed and "skew" EPR transitions are given. Results at zero external field are given in the text, Eq. (6.27).

$\|i\rangle$	$\|j\rangle$	t_3^{ij} ($\text{sec}^{-1}\,\text{K}^{-1}$)	Direct process t_4^{ij} ($\text{sec}^{-1}\,\text{K}^{-1}$)	t_5^{ij} ($\text{sec}^{-1}\,\text{K}^{-1}$)	Raman process T^{ij}/T^9 ($10^{-5}\,\text{sec}^{-1}\,\text{K}^{-9}$)	Orbach process $\Delta\Gamma_7=30.1\ \text{cm}^{-1}$ $T^{ij}/e^{-\Delta/kT}$ ($10^8\ \text{sec}^{-1}$)	Orbach process $\Delta\Gamma_8=33.5$ cm $T^{ij}/e^{-\Delta/kT}$ ($10^8\ \text{sec}^{-1}$)
|44⟩	|33⟩	0	9.32	169.04	11.88	10.26	66.50
|44⟩	|32⟩	24.38	0	7.71	0	0	0
|43⟩	|33⟩	71.41	0.41	0	0.97	0.53	3.42
|43⟩	|32⟩	0	6.73	97.16	17.87	9.73	63.04
|43⟩	|31⟩	34.25	0	10.83	0	0	0
|42⟩	|33⟩	0	0.01	1.56	0.03	0.01	0.09
|42⟩	|32⟩	94.20	0.61	0	1.91	1.04	6.75
|42⟩	|31⟩	0	4.62	50.98	16.89	9.19	59.56
|42⟩	|30⟩	34.01	0	10.76	0	0	0
|41⟩	|32⟩	0	0.02	3.27	0.08	0.04	0.28
|41⟩	|31⟩	87.10	0.64	0	2.83	1.54	9.98
|41⟩	|30⟩	0	2.96	23.59	15.90	8.60	56.08
|41⟩	|3−1⟩	27.58	0	8.72	0	0	0
|40⟩	|32⟩	0.23	0	0.07	0	0	0
|40⟩	|31⟩	0	0.03	4.25	0.17	0.09	0.58
|40⟩	|30⟩	65.13	0.56	0	3.71	2.02	13.10
|40⟩	|3−1⟩	0	1.71	9.11	14.92	8.13	52.63
|40⟩	|3−2⟩	18.37	0	5.81	0	0	0
|4−1⟩	|4−3⟩	0.12	0	0.03	0	0	0
|4−1⟩	|31⟩	0.37	0	0.12	0	0	0
|4−1⟩	|30⟩	0	0.03	4.14	0.28	0.02	1.00
|4−1⟩	|3−1⟩	39.63	0.40	0.0	4.55	2.48	16.04
|4−1⟩	|3−2⟩	0	0.84	2.67	13.99	7.62	49.35
|4−1⟩	|3−3⟩	9.28	0	2.94	0	0	0
|4−2⟩	|4−4⟩	2.44	0	0.77	0	0	0
|4−2⟩	|30⟩	0.43	0	0.14	0	0	0
|4−2⟩	|3−1⟩	0	0.03	3.03	0.43	0.23	1.51
|4−2⟩	|3−2⟩	18.25	0.22	0	5.28	2.88	18.64
|4−2⟩	|3−3⟩	0	0.30	0.53	13.28	7.23	46.83
|4−3⟩	|4−4⟩	0	0.03	0.12	15.87	8.64	55.96
|4−3⟩	|3−1⟩	0.32	0	0.10	0	0	0
|4−3⟩	|3−2⟩	0	0.01	1.41	0.59	0.31	2.01
|4−3⟩	|3−3⟩	4.95	0.07	0	5.71	3.11	20.16
|4−4⟩	|3−2⟩	0.21	0	0.07	0	0	0
|4−4⟩	|3−3⟩	0	0	0.18	3.49	1.90	12.29

Owing to the very large magnetic hyperfine interaction in this system, relaxation at moderate external fields ($H<10$ kG) occurs generally in a multiexponential manner.

Huang[6] measured the spin-lattice relaxation of a sample of 0.02-mole% Ho^{2+} in CaF_2 with an external magnetic field along the crystal [100] direction. The result of his pulse-saturation experiment of the $|4-4\rangle \rightarrow |4-3\rangle$ transition (see Fig. 2) was fit by the inverse relaxation time

$$1/T_1 = 42T + 8.0\times10^9\, e^{-47.6/T} \quad . \tag{6.28}$$

Table IX gives a large relaxation rate for the $|4-4\rangle \rightarrow |4-3\rangle$ transition and indicates that resonant Raman relaxation via the Γ_8 electronic level for this transition will occur with an approximately single exponential decay characterized by

$$1/T_1 = 1.1\times10^{10}\, e^{-48.2/T} \tag{6.29}$$

in rather good agreement with experiment. Raman relaxation and resonant Raman relaxation via the Γ_7 electronic level are seen to be generally smaller than the Γ_8 resonant Raman relaxation, or at low temperatures, the direct process. Direct-process relaxation under the experimental conditions, is a sum of exponential decays, owing to the large hyperfine constant for this system. Diagonalizing the direct-process reduced transition-rate matrix

and calculating the time evolution of the system following a short saturating pulse applied to the $|4-4\rangle \rightarrow |4-3\rangle$ transition reveals that the dominant exponentials in the return of the system to equilibrium are $3.6T$ and $4.5T$, about an order of magnitude smaller than the measured direct-process relaxation time.

C. MgO : Er^{3+}

One of the few cases in which a Γ_8 quartet electronic ground level occurs is the system MgO : Er^{3+}. The existence of two electronic Kramers doublets in the ground manifold provides a complex and challenging system for spectroscopic and relaxation studies. Belorizky *et al.*[35] have provided a detailed EPR study of the hyperfine structure in this system. From EPR results Descamps and d'Aubigné[36] have determined approximate crystal-field parameters for the system, indicating the existence of an excited Γ_7 doublet at about 110 cm^{-1} and an excited Γ_8 quartet at approximately 140 cm^{-1}.

The spin Hamiltonian ($\tilde{S}=\frac{3}{2}$) for a Γ_8 quartet is quite complex:

$$\mathcal{H}_s = g\mu_\beta \vec{H}\cdot\vec{\tilde{S}} + u\mu_\beta\{\tilde{S}_x^3 H_x + \tilde{S}_y^3 H_y + \tilde{S}_z^3 H_z - \tfrac{1}{5}(\vec{\tilde{S}}\cdot\vec{H})[3\tilde{S}(\tilde{S}+1)-1]\} + A\vec{I}\cdot\vec{\tilde{S}}$$
$$+ U\{\tilde{S}_x^3 I_x + \tilde{S}_y^3 I_y + \tilde{S}_z^3 I_z - \tfrac{1}{5}(\vec{\tilde{S}}\cdot\vec{I})[3\tilde{S}(\tilde{S}+1)-1]\} + B\frac{m}{6}\sum_{q=1}^{3}[3I_q^2 - I(I+1)][3\tilde{S}_q^2 - \tilde{S}(\tilde{S}+1)]$$
$$+ B\frac{3n}{4}\sum_{p\neq q}(I_pI_q + I_qI_p)(\tilde{S}_p\tilde{S}_q + \tilde{S}_q\tilde{S}_p) \quad . \qquad (6.30)$$

The first and second terms in Eq. (6.30) represent the electronic Zeeman interaction, while the third and fourth terms correspond to the magnetic hyperfine interaction. The remaining terms describe the nuclear quadrupole interaction with the paramagnetic electrons. Nuclear Zeeman and pseudonuclear Zeeman terms for MgO : Er^{3+} are small and have been deleted from Eq. (6.30). A full discussion of this spin Hamiltonian has been provided by Abragam and Bleaney.[23] The parameters of Belorisky *et al.*[35] will be employed in the following calculations.

Since U in Eq. (6.30) is much smaller than A for the system, at zero field the quantity

$$\vec{F} = \vec{\tilde{S}} + \vec{I}$$

is approximately a good quantum number. Zero-field energy levels fall into groups of 5, 7, 9, and 11 states corresponding to $F=2, 3, 4$, and 5, respectively. There are 13 distinct energy levels at zero field transforming as $\Gamma_1+\Gamma_2+3\Gamma_3+4\Gamma_4+4\Gamma_5$ in the cubic group. A convenient labeling scheme for zero-field hyperfine states is provided by F and the irreducible representation Γ. Energy levels at zero field are given in Table X.

Energy levels at a representative value of a strong magnetic field $H=1.4$ kG along a crystal [100] axis are depicted in Fig. 3. A direct-product $|M_{\tilde{S}}\ M_I\rangle$ notation is more appropriate for labeling the high-field states.

1. Direct process

Direct-process relaxation rates (3.33) were computed at zero field employing $v_L = 8.94\times10^5$ cm/sec^{-1} and $v_T = 6.43\times10^5$ cm/sec^{-1}.[37] Unlike the preceding systems, with Kramers-doublet ground states, in the present case

$$\langle j|\ V(\Gamma\beta)\ |i\rangle \neq 0 \quad ,$$

when $|j\rangle$ and $|i\rangle$ are zeroth-order hyperfine states.

The matrix element does not vanish because the $|\pm\frac{3}{2}\rangle$ and $|\pm\frac{1}{2}\rangle$ electronic states both appear to some extent in the hyperfine wave function. Representative values of the direct process $\bar{W}_{kl}^{lev}$ at zero field are given in Table XI. From the symmetries of the levels involved, the lattice modes contributing to the relaxation may be found.

Direct-process reduced transition rates for

TABLE X. Energy levels and state designations for MgO : Er^{3+} at zero field [see discussion following Eq. (6.30)]. Uncertainty in energy levels is approximately ±30 MHz due to experimental uncertainty in spin-Hamiltonian parameters.

F	Γ	Energy (MHz)
2	Γ_3	2577
2	Γ_5	2569
3	Γ_2	1703
3	Γ_5	1659
3	Γ_4	1626
4	Γ_5	181
4	Γ_3	113
4	Γ_4	83
4	Γ_1	37
5	$\Gamma_{4,a}$	−2168
5	Γ_5	−2237
5	Γ_3	−2434
5	$\Gamma_{4,b}$	−2463

some allowed and skew EPR transitions at 1.4 kG are given in Table XII. The largest rates correspond to $|\pm\frac{3}{2}M_I\rangle \rightarrow |\pm\frac{1}{2}M_I\rangle$ transitions, owing to the non-Kramers-conjugate nature of the electronic states involved.

2. *Raman process*

Raman relaxation rates were calculated employing Eqs. (3.38)–(3.41). Since the ground multiplet is derived from four electronic states and not a simple Kramers pair, temperature dependences from T^5 to T^9 will in general occur. Semidiagonal matrix elements of $\mathcal{H}_{11}$, i.e., matrix elements of the form

$$\langle M_{\tilde{S}} N | \mathcal{H}_{11} | M_{\tilde{S}} N \pm 1\rangle \tag{6.31}$$

make a nonvanishing contribution to the T^5 and T^6 terms and have been included in the calculation.[38] It should be mentioned that in addition to the Raman processes arising from second-order perturbation theory the third term in the Taylor expansion (5.2), namely,

$$\sum_{j\,l\,\Gamma\alpha\beta} \frac{4\pi e Q_j}{2l+1} (\delta\vec{R}_j - \delta\vec{R}_0)(\delta\vec{R}_j - \delta\vec{R}_0): \times\left(\vec{\nabla}_{(\vec{R}_j-\vec{R}_0)}\vec{\nabla}_{(\vec{R}_j-\vec{R}_0)} \times \frac{Y^*(l\,\Gamma\alpha\beta;\theta_j\varphi_j)}{|\vec{R}_j-\vec{R}_0|^{l+1}}\right)_{(\vec{R}_j^0-\vec{R}_0^0)} r^l Y(l\,\Gamma\alpha\beta;\theta,\varphi) \tag{6.32}$$

gives rise to a similar Raman process in first-order perturbation theory, significant only when initial and final states are not simply derived from a Kramers-conjugate pair. Contributions from (6.32) to the Raman relaxation have been neglected in the present calculations, but should be included in a more refined treatment of this system.

Representative values of the Raman process $\tilde{W}_{kl}^{\text{lev}}$ at zero field are expressed as a power series

$$\tilde{W}_{kl}^{\text{lev}}(\text{Raman}) = \tilde{W}_{kl}^{\text{lev}}(R5)T^5 + \tilde{W}_{kl}^{\text{lev}}(R6)T^6 + \tilde{W}_{kl}^{\text{lev}}(R7)T^7 + \tilde{W}_{kl}^{\text{lev}}(R8)T^8 + \tilde{W}_{kl}^{\text{lev}}(R9)T^9 \tag{6.33}$$

and are included in Table XI. It becomes apparent that zero-field transitions among the hyperfine levels of this system might be divided into three categories. For such transitions as $(2\Gamma_3) \rightarrow (5\Gamma_5)$, the relaxation resembles that of a Kramers doublet, with small direct process and T^5 and T^9 terms dominant in Raman relaxation. For the $(2\Gamma_3) \rightarrow (4\Gamma_1)$ and similar transitions, relaxation resembles that of a time even (non-Kramers) doublet with large direct process and a T^7 Raman process. Lastly, for the $(2\Gamma_3) \rightarrow (3\Gamma_5)$ and many other transitions, a moderate direct process and T^5 through T^9 Raman process are observed. In all cases the "cross terms" with T^6 and T^8 dependences are smaller than the T^5, T^7, and T^9 terms.

Values of the Raman process T^{ij} $(= \tilde{W}_{ij}^{\text{lev}})$ for some allowed and skew EPR transitions at 1.4 kG are included in Table XII. The Van Vleck cancellation is readily apparent in the $|M_{\tilde{S}}M_I\rangle \rightarrow |-M_{\tilde{S}}M_I\rangle$ transitions. The $|\pm\frac{3}{2}M_I\rangle \rightarrow |\pm\frac{1}{2}M_I\rangle$ display not only a dominant T^7 Raman relaxation but also T^5 and T^9 processes.

Relaxation rates for resonant Raman processes via the Γ_7 level at 110 cm^{-1} and the Γ_8 level at 140 cm^{-1} are included in Table XI for zero field and Table XII for $H = 1.4$ kG. Resonant Raman relaxation is significant for almost all transitions at zero field and for allowed EPR transitions (including $\Delta M_{\tilde{S}} = 2$) at high field.

3. *Summary and comparison with experiment*

The direct relaxation process for MgO: Er^{3+} is seen from Tables XI and XII to be dominant in the low-temperature ($T \leq 10$ K) region. Relaxation among hyperfine levels is expected to be quite complex, particularly at zero field. In general, a multiexponential return to equilibrium is to be expected.

Relaxation among hyperfine levels in this system has not yet been studied experimentally. The calculated results for allowed EPR transitions

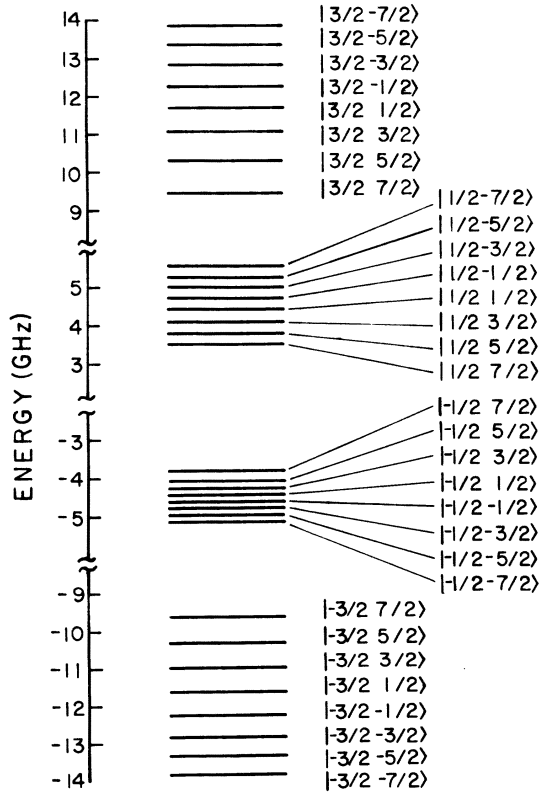

FIG. 3. Hyperfine energy levels of $^{167}Er^{3+}$ in MgO with $H = 1.4$ kG along a crystal [100] axis.

might be compared with the experimental measurements of Borg, Buisson, and Jacolin[10] on MgO: Er^{3+} with zero nuclear spin. Borg *et al.* found the direct process to be dominant in the liquid-helium range and obtained principal direct-process rates within a factor of 4 of the analogous rates in our calculation. Raman relaxation was not detected in their experiment. Calculated Raman rates given in this paper are more than an order of magnitude larger than those calculated by Borg *et al.* This disagreement is entirely attributed to the choice of an unshielded value of $\langle r^2 \rangle$ in the present calculations. However, even the larger calculated values given here do not predict an observable Raman process below 4.2 K.

VII. DISCUSSION AND CRITIQUE

We have presented an analysis of spin-lattice relaxation among hyperfine levels of a paramagnetic ion located at a site of cubic (O_h) symmetry in a diamagnetic host. Our approach has centered on a formulation of lattice continuum dynamics in terms of "spherical waves" and a thorough application of symmetry considerations to all aspects of the problem.

We believe the spherical wave approach to be a promising alternative to more traditional approaches, more amenable to the physical intuition, and of great value in treating more realistic models for the spin-lattice relaxation phenomenon. Reasonable goals for spin-lattice relaxation theory at the present time would certainly include (i) providing the investigator with a set of viable concepts for understanding the phenomenon on a pictorial level, and (ii) formulating a computational scheme to obtain reliable predictions of relaxation behavior based on a few readily obtainable spectroscopic and elastic parameters. We believe the spherical wave approach contributes substantially to these goals.

Conceptually, the spherical wave approach allows treatment of ion wave functions and lattice modes on an equal footing. Ion states and lattice states transforming as irreducible representations of the ion site symmetry group are formed in an identical manner and the ion-lattice interaction, which must transform as the totally symmetric representation of the site group takes on a particularly simple form. Since only a few lattice modes possess substantial intensity near the origin, the ion is coupled to only a small number of lattice modes. Use of spherical modes also facilitates the visualization and mathematical analysis of the acoustic radiation pattern of a relaxing ion.

Since phonons involved in spin-lattice relaxation typically possess wavelengths extending over many unit cells of the lattice, the use of a continuum model is far more easily dealt with computationally

TABLE XI. Elements of the reduced transition-rate matrix $\tilde{W}^{lsr}$ for MgO: Er^{3+} at zero field separated into contributions from the direct, Raman, and resonant-Raman processes. Only matrix elements for transitions from the $(2\Gamma_3)$ level are given, as representative of the entire 13×13 matrix. Raman rates are separated into contributions with $T^n (n = 5, \ldots, 9)$ temperature dependences $\tilde{W}^{lsr}(\text{Raman}) = \tilde{W}^{lsr}(R5)\, T^6 + \tilde{W}^{lsr}(R6)\, T^6 + \tilde{W}^{lsr}(R7)\, T^7 + \tilde{W}^{lsr}(R8)\, T^8 + \tilde{W}^{lsr}(R9)\, T^9$.

k ($F\Gamma$)	l ($F\Gamma$)	Direct process $\tilde{W}^{lsr}_{kl}/T$ ($\text{sec}^{-1}\,\text{K}^{-1}$)	Raman processes $\tilde{W}^{lsr}_{kl}(R5)$ ($10^{-3}\,\text{sec}^{-1}\,\text{K}^{-5}$)	$\tilde{W}^{lsr}_{kl}(R6)$ ($10^{-12}\,\text{sec}^{-1}\,\text{K}^{-6}$)	$\tilde{W}^{lsr}_{kl}(R7)$ ($10^{-6}\,\text{sec}^{-1}\,\text{K}^{-7}$)	$\tilde{W}^{lsr}_{kl}(R8)$ ($10^{-15}\,\text{sec}^{-1}\,\text{K}^{-8}$)	$\tilde{W}^{lsr}_{kl}(R9)$ ($10^{-9}\,\text{sec}^{-1}\,\text{K}^{-9}$)	Resonant-Raman processes $\Delta = 110\ \text{cm}^{-1}$ $\tilde{W}^{lsr}_{kl}/e^{-\Delta/kT}$ ($10^{9}\,\text{sec}^{-1}$)	$\Delta = 140\ \text{cm}^{-1}$ $\tilde{W}^{lsr}_{kl}/e^{-\Delta/kT}$ ($10^{9}\,\text{sec}^{-1}$)
$(2\Gamma_3)$	$(2\Gamma_5)$	0	0.463	−0.067	0.096	0.543	11.474	4.252	4.181
	$(3\Gamma_2)$	0.283	0	−0.014	5.939	0	0	1.815	3.507
	$(3\Gamma_5)$	2.106	0.446	0.213	0.755	−1.118	7.225	3.698	11.369
	$(3\Gamma_4)$	0.449	0.240	1.054	0.150	0.125	8.256	4.108	4.944
	$(4\Gamma_5)$	10.215	0.453	3.260	0.538	3.675	0.803	1.369	8.932
	$(4\Gamma_3)$	0.229	0.005	−0.011	6.045	0	0.001	1.871	3.707
	$(4\Gamma_4)$	25.362	0.024	−0.731	1.232	−7.740	0.084	2.775	15.617
	$(4\Gamma_1)$	2.388	0	0	5.938	0	0	1.815	3.498
	$(5\Gamma_4a)$	0.190	1.515	−0.120	0.003	−0.345	2.752	0.458	7.274
	$(5\Gamma_5)$	0	0.712	0.008	0	0.047	1.537	0.338	3.059
	$(5\Gamma_3)$	0.063	0.019	−0.018	0.040	0	0.002	0.105	0.606
	$(5\Gamma_4b)$	0.343	0.295	0.073	0.041	−0.389	0.771	0.195	1.165

TABLE XII. Direction-corrected transition rates $T^{ij}(=\tilde{W}^{lev}_{ij})$ for $MgO:Er^{3+}$ at $H=1.4$ kG along a crystal [100] axis. Rates are separated into direct, Raman, and resonant-Raman contributions. Raman rates are separated into contributions with T^n ($n=5, \ldots, 9$) temperature dependences. $T^{ij}_{\text{Raman}} = t^{ij}_{R5}T^5 + t^{ij}_{R6}T^6 + t^{ij}_{R7}T^7 + t^{ij}_{R8}T^8 + t^{ij}_{R9}T^9$. Representative rates for allowed and skew EPR transition are given.

$\|i\rangle$	$\|j\rangle$	Direct process T^{ij}/T ($\text{sec}^{-1}\text{K}^{-1}$)	Raman processes t^{ij}_{R5} (10^{-3} $\text{sec}^{-1}\text{K}^{-5}$)	t^{ij}_{R6} (10^{-12} $\text{sec}^{-1}\text{K}^{-6}$)	t^{ij}_{R7} (10^{-6} $\text{sec}^{-1}\text{K}^{-7}$)	t^{ij}_{R8} (10^{-15} $\text{sec}^{-1}\text{K}^{-8}$)	t^{ij}_{R9} (10^{-9} $\text{sec}^{-1}\text{K}^{-9}$)	Resonant-Raman processes $\Delta=110$ cm^{-1} $T^{ij}/e^{-\Delta/kT}$ (10^9 sec^{-1})	$\Delta=140$ cm^{-1} $T^{ij}/e^{-\Delta/kT}$ (10^9 sec^{-1})
$\|\frac{3}{2}\ \frac{7}{2}\rangle$	$\|\frac{1}{2}\ \frac{7}{2}\rangle$	1010.4	0.696	27.440	4.453	5.995	17.623	20.050	66.728
	$\|-\frac{1}{2}\ \frac{5}{2}\rangle$	51.4	0.052	0.089	0.044	0.319	0.112	0.122	0.780
	$\|-\frac{1}{2}\ \frac{7}{2}\rangle$	3050.8	0.379	−9.636	18.137	−5.323	1.164	10.500	40.127
	$\|-\frac{3}{2}\ \frac{5}{2}\rangle$	22.5	0.022	−0.039	0.065	−0.389	0.068	0.072	0.263
	$\|-\frac{3}{2}\ \frac{7}{2}\rangle$	0	6.017	−0.003	0	−0.026	11.341	20.614	28.171
$\|\frac{1}{2}\ \frac{7}{2}\rangle$	$\|-\frac{1}{2}\ \frac{5}{2}\rangle$	0	0.115	0	0	0	0.025	0.107	0.788
	$\|-\frac{1}{2}\ \frac{7}{2}\rangle$	0.4	5.873	0.062	0.001	0.389	60.105	13.460	19.850
	$\|-\frac{3}{2}\ \frac{5}{2}\rangle$	52.0	0.138	−0.088	0.044	−0.416	0.618	0.191	1.050
	$\|-\frac{3}{2}\ \frac{7}{2}\rangle$	3155.1	0.397	4.884	18.029	6.217	1.219	10.467	39.979
$\|-\frac{1}{2}\ \frac{5}{2}\rangle$	$\|-\frac{1}{2}\ \frac{7}{2}\rangle$	0	0.073	−0.938	0.095	−0.347	0.093	0.260	1.563
	$\|-\frac{3}{2}\ \frac{5}{2}\rangle$	987.8	0.662	−18.636	4.228	−4.663	17.113	19.162	63.380
	$\|-\frac{3}{2}\ \frac{7}{2}\rangle$	6.7	0.004	0.048	0.017	0.389	0.013	0.103	0.399
$\|-\frac{1}{2}\ \frac{7}{2}\rangle$	$\|-\frac{3}{2}\ \frac{5}{2}\rangle$	5.7	0.229	0	1.362	0	1.243	0.586	1.642
	$\|-\frac{3}{2}\ \frac{7}{2}\rangle$	1102.4	0.693	−26.021	4.433	−6.661	17.027	19.782	66.401

than any discrete model sufficiently detailed to account for the measured lattice spectrum. Thus, it would seem that the use of continuum models in routine spin-lattice relaxation calculations is reasonable and the development of modified more realistic continuum models should be investigated.

Future investigations will approach the problem of spin-lattice relaxation in anisotropic systems, employing a lattice potential energy density function suited to the actual lattice symmetry. Lattice vibrational modes might be constructed by perturbation techniques from a basis set of spherical modes. Only the coefficients of the (angular momentum) $n=0$, 1, 2 modes in the resulting perturbation series need be determined, together with a dispersion relation and density of states function for the modes involved in spin-lattice relaxation. The lattice dynamical problem cast in a spherical mode basis set may lead to effective approximation schemes for a more realistic model of relaxation phenomenon.

Further work will also investigate the adaptation of a continuum model to incorporate the mass and force constant perturbations associated with the impurity ion. The geometry of the point impurity problem suggests that a spherical mode treatment is appropriate and that the resulting perturbed density of states will take on a particularly simple form.

It has been shown that the spin-lattice relaxation rate expressions are most simply derived when lattice modes are chosen to transform as rows of the irreducible representation of the paramagnetic ion site group. Total relaxation rates have been separated into contributions associated with lattice modes of different symmetries, making possible a more detailed comparison of theory with experiment.

Relaxation rates have been calculated for hyperfine levels of the systems $CaF_2:Tm^{2+}$, $CaF_2:Ho^{2+}$, and $MgO:Er^{3+}$, based on a point-charge dynamical crystal-field model and isotropic elastic continuum-lattice dynamics. Symmetry considerations have been employed to minimize the number of independent coefficients in the ion-lattice interaction Hamiltonian.

The systems $CaF_2:Tm^{2+}$ and $CaF_2:Ho^{2+}$ with Kramers-doublet electronic ground levels display a small direct process and T^9 Raman process. In order to treat relaxation between levels not derived from a simple time reversed pair of electronic states, a completely general derivation of the Raman relaxation rate is given with temperature dependence being a sum of terms T^n ($n=5,\ldots,9$). The more general analysis of the Raman process is directly applicable to $MgO:Er^{3+}$ which has a Γ_8 quartet electronic ground level. The direct process in $MgO:Er^{3+}$ however, is shown to be much larger than in the electronic Kramers-doublet system and to dominate relaxation below 10 K.

APPENDIX: LATTICE DYNAMICS IN A PLANE-WAVE BASIS

It is of course possible to construct linear combinations of plane-wave normal modes transforming as rows of the irreducible representations of the cubic group. While two standard methods exist for such constructions, we have devised a novel method for forming the appropriate linear combinations which is particularly well suited to treatment of the spin-lattice interaction *in the long-wavelength approximation* (3.7).

Assuming that $\vec{s}(\vec{r})$ satisfies periodic boundary conditions over a cube of side L, one obtains one longitudinal and two transverse families of normal mode solutions to (2.9). To illustrate the various methods, the longitudinal solutions

$$\vec{s}_{L\vec{k}} = (\vec{k}/L^3 k)\, e^{i\vec{k}\cdot\vec{r}} \tag{A1}$$

are employed. Components of $\vec{k}$ are given by

$$k_i = 2\pi n_i/L\ , \quad n_i = 0, \pm 1, \ldots, \tag{A2}$$

with $\vec{k}$ restricted to the first Brillouin zone. For general $\vec{k}$, $\vec{s}_{L\vec{k}}$ is degenerate with $\vec{s}_{L\vec{k}'}$ when $\vec{k}$ and $\vec{k}'$ are related by a site-group operation. The set of wave vectors so related is conventionally designated k^*. For the cubic group k^* will contain 48 vectors. From the 48 associated normal modes linear combinations may be formed[39] transforming as $\Gamma_{1g}+\Gamma_{2g}+2\Gamma_{3g}+3\Gamma_{4g}+3\Gamma_{5g}+\Gamma_{1u}+\Gamma_{2u}+2\Gamma_{3u}+3\Gamma_{4u}+3\Gamma_{5u}$.

Such linear combinations may be formed using the projection operators[40]

$$\mathcal{P}^{(j)}_{\beta\beta} = \frac{l_j}{48}\sum_R [\Gamma^{(j)}(R)]^*_{\beta\beta} P_R\ , \tag{A3}$$

which when applied to $\vec{s}_{L\vec{k}}$ generate linear combinations of $\vec{s}_{L\vec{k}'}$, ($\vec{k}'\in k^*$) transforming as the βth row of the jth irreducible representation of the cubic group. In Eq. (A3), l_j is the dimensionality of the jth representation, $\Gamma^{(j)}_{\beta\beta}$ is the diagonal element of the βth row of the matrix representation $\Gamma^{(j)}$ of the group element R, and the sum runs over all the symmetry elements of the group. P_R is an operation on functions of position defined by

$$P_R f(\vec{r}) = f(R^{-1}\vec{r})\ . \tag{A4}$$

There are, for the group O_h, 20 projection operators $\mathcal{P}^{(j)}_{\beta\beta}$ corresponding to all rows of the 10 representations. Applying the 20 $\mathcal{P}^{(j)}_{\beta\beta}$ to $\vec{s}_{L\vec{k}}$ will thus generate 20 different normal modes each transforming as a row of an irreducible representation of the cubic group. To obtain the additional 28 independent normal modes transforming as rows of the degenerate representations, it is necessary to apply $\mathcal{P}^{(j)}_{\beta\beta}$ to a second and third plane-wave mode $\vec{s}_{L\vec{k}'}$,

$\vec{s}_{L\vec{k}''}$ associated with k^*. Unfortunately, the normal modes constructed from $\vec{s}_{L\vec{k}'}$, and $\vec{s}_{L\vec{k}''}$ will not necessarily be orthogonal to the mode of the same symmetry constructed from $\vec{s}_{L\vec{k}}$. The Gram-Schmidt or other orthogonalization procedure must then be used to complete the set of 48 independent normal modes. Further, the two or three linear combinations transforming as the same row of a degenerate representation will in general all make a nonzero contribution to the corresponding $\sigma_0(\Gamma\beta)$ [Eq. (3.6)].

The second standard method[39] employed in forming linear combinations of plane waves involves the "cubic" harmonics $Y(l\Gamma a\beta;\theta\varphi)$ [Eq. (2.30)]. It can be verified that the function

$$s_{Lk^*l\Gamma a\beta}=\sum_{\vec{k}\in k^*} Y(l\Gamma a\beta;\theta_{\vec{k}}\varphi_{\vec{k}})s_{L\vec{k}} \tag{A5}$$

transforms as the βth row of the irreducible representation Γ. This method presents difficulties similar to that of the projection operators (A3). To obtain the two or three normal modes corresponding to a row of a degenerate representation, cubic harmonics of different l or a must be employed. The resulting functions are not necessarily orthogonal and even the orthonormalized linear combinations which must then be constructed will all make nonvanishing contributions to $\sigma_0(\Gamma\beta)$.

The following new method is an application of elementary Hilbert space theory to the normal modes (A1). The set $\mathfrak{L}(k^*)$ of all linear combinations of normal modes $\vec{s}_{L\vec{k}}$, $(\vec{k}\in k^*)$ forms a Hilbert space with the scalar product

$$(\vec{f},\vec{g})=\int_{-L/2}^{L/2}\int_{-L/2}^{L/2}\int_{-L/2}^{L/2}\vec{f}^*\cdot\vec{g}\,dx\,dy\,dz\ . \tag{A6}$$

Related to the nine cubic strain tensor components $\sigma_0(\Gamma\beta)$ [Eq. (3.6)] are a family of nine linear transformations $\sigma_{\Gamma\beta}$ from the Hilbert space $\mathfrak{L}(k^*)$ to the set of complex numbers, such that $\sigma_{\Gamma\beta}(\vec{f})$ is the contribution of the function $\vec{f}$ to the strain component $\sigma_0(\Gamma\beta)$. Thus,

$$\begin{aligned}
\sigma_{\Gamma_{1g}}(\vec{f})&=-\frac{1}{\sqrt{3}}\left(\frac{\partial f_x}{\partial x}+\frac{\partial f_y}{\partial y}+\frac{\partial f_z}{\partial z}\right)_{\vec{r}=\vec{0}},\\
\sigma_{\Gamma_{4g}0}(\vec{f})&=\frac{i}{\sqrt{2}}\left(\frac{\partial f_y}{\partial x}-\frac{\partial f_x}{\partial y}\right)_{\vec{r}=\vec{0}},\\
\sigma_{\Gamma_{3g}\epsilon}(\vec{f})&=\frac{1}{\sqrt{2}}\left(\frac{\partial f_x}{\partial x}-\frac{\partial f_y}{\partial y}\right)_{\vec{r}=\vec{0}},
\end{aligned} \tag{A7}$$

and so on. Each of the $\sigma_{\Gamma\beta}$ is a linear functional[41] on $\mathfrak{L}(k^*)$. According to the Reisz lemma, for each linear functional $\sigma_{\Gamma\beta}$, there is a unique function $\vec{y}_{\Gamma\beta}$ belonging to $\mathfrak{L}(k^*)$ such that

$$\sigma_{\Gamma\beta}(\vec{f})=(\vec{y}_{\Gamma\beta},\vec{f}) \tag{A8}$$

for all $\vec{f}$ in $\mathfrak{L}(k^*)$. It immediately follows that if $\vec{g}$ is orthogonal to $\vec{y}_{\Gamma\beta}$,

$$\sigma_{\Gamma\beta}(\vec{g})=0\ .$$

Since the set of longitunal modes $\{\vec{s}_{L\vec{k}};\vec{k}\in k^*\}$ forms an orthornormal basis for the Hilbert space $\mathfrak{L}(k^*)$, the function $\vec{y}_{\Gamma\beta}$ can be written as the sum of projections onto these basis functions

$$\vec{y}_{\Gamma\beta}=\sum_{k\in k^*}\vec{s}_{L\vec{k}}(\vec{s}_{L\vec{k}},\vec{y}_{\Gamma\beta})\ . \tag{A9}$$

Employing Eq. (A8) the above expansion may be written

$$\vec{y}_{\Gamma\beta}=\sum_{\vec{k}\in k^*}\vec{s}_{L\vec{k}}\sigma^*_{\Gamma\beta}(\vec{s}_{L\vec{k}})\ . \tag{A10}$$

From Eqs. (A10), (A7), and (A1) the functions $\vec{y}_{\Gamma\beta}$ may be evaluated.

It follows from the transformation properties of the $\vec{y}_{\Gamma\beta}$ that

$$(\vec{y}_{\Gamma\beta},\vec{y}_{\Gamma'\beta'})=0\ ,$$

unless $\Gamma=\Gamma'$ and $\beta=\beta'$. The $\vec{y}_{\Gamma\beta}$ are not normalized with respect to Eq. (A6), however normalized functions $\vec{s}_{Lk^*\Gamma\beta}$ proportional to $\vec{y}_{\Gamma\beta}$ are quite easily constructed:

$$\vec{s}_{Lk^*\Gamma\beta}=\vec{y}_{\Gamma\beta}/(\vec{y}_{\Gamma\beta},\vec{y}_{\Gamma\beta})^{1/2}\ . \tag{A11}$$

In forming linear combinations of the 48 normal modes $\{\vec{s}_{L\vec{k}};\vec{k}\in k^*\}$ to transform as rows of the irreducible representations of the group O_h it is desired to minimize the number of independent normal modes with nonvanishing cubic strain components at the origin. Since it follows directly from the Reisz lemma that any linear combination of modes orthogonal to $\vec{s}_{Lk^*\Gamma\beta}$ will make no contribution to the strain component $\sigma_0(\Gamma\beta)$, if the transformed set of normal modes is chosen to contain the functions $\vec{s}_{Lk^*\Gamma\beta}$ only these nine functions will possess nonvanishing strain. Actually only six of the $\vec{s}_{Lk^*\Gamma\beta}$ need be considered since $\sigma_0(\Gamma_{4g},\beta)=0$ for longitudinal modes. Inserting (A11) in place of $\vec{f}$ in Eq. (A8) it is seen that the nonzero strain component associated with $\vec{s}_{Lk^*\Gamma\beta}$ is

$$\sigma_0(\Gamma\beta)=(\vec{y}_{\Gamma\beta},\vec{y}_{\Gamma\beta})^{1/2}\ . \tag{A12}$$

An identical analysis may be applied to both families of transverse normal modes associated with k^* resulting in a set of 96 transverse modes of which only eight possess nonvanishing strain.

We have derived relaxation-rate expressions for direct and Raman processes using the strains (A12) and the restricted density of states

$$\rho_{Xk^*\Gamma\beta}=\tfrac{1}{48}L^3/8\pi^3\ . \tag{A13}$$

The results obtained are identical to those for the spherical mode approach described in this paper.

*Work supported in part by the Office of Naval Research, U. S. Army Research Office, Durham, and National Science Foundation.

†National Science Foundation Predoctoral Fellow 1969–1972.

[1]*Spin-Lattice Relaxation in Ionic Solids*, edited by A. A. Manenkov and R. Orbach (Harper and Row, New York, 1966).

[2]R. Orbach, Proc. R. Soc. A 264, 456 (1961).

[3]P. L. Scott and C. D. Jeffries, Phys. Rev. 127, 32 (1962).

[4]J. H. Van Vleck, Phys. Rev. 57, 426 (1940).

[5]R. Buisson and M. Borg, Phys. Rev. B 1, 3577 (1970).

[6]C. Y. Huang, Phys. Rev. 139, A241 (1965).

[7]G. E. Stedman and D. J. Newman, J. Chem. Phys. 55, 152 (1971).

[8]K. W. H. Stevens, Rept. Prog. Phys. 30, 189 (1967).

[9]E. R. Bernstein and D. R. Franceschetti, Phys. Rev. B 6, 1654 (1972).

[10]M. Borg, R. Buisson, and C. Jacolin, Phys. Rev. B 1, 1917 (1970).

[11]A. Abragam, J. F. Jacquinot, M. Chapelier, and M. Goldman, J. Phys. C 5, 2629 (1972).

[12]E. R. Bernstein and G. M. Dobbs (unpublished).

[13]U. Fano and G. Racah, *Irreducible Tensorial Sets* (Academic, New York, 1959).

[14]C. Kittel, *Quantum Theory of Solids* (Wiley, New York, 1963), p. 21.

[15]H. B. Huntington, Solid State Phys. 7, 214 (1958).

[16]P. M. Morse and H. Feshbach, *Methods of Theoretical Physics* (McGraw-Hill, New York, 1953), Vol. I, p. 345.

[17]P. Debye, Ann. Phys. (Leipzig) 39, 789 (1912).

[18]A. R. Edmonds, *Angular Momentum in Quantum Mechanics*, 2nd ed. (Princeton U. P., Princeton, N. J., 1960), p. 81ff.

[19]J. S. Griffith, *Theory of Transition Metal Ions* (Cambridge U. P., London, 1971), p. 393ff.

[20]I. S. Gradshteyn and I. W. Ryzhik, *Tables of Integrals Series and Products* (Academic, New York, 1965), p. 352.

[21]R. Orbach and M. Blume, Phys. Rev. Lett. 8, 478 (1962).

[22]W. Heitler, *Quantum Theory of Radiation*, 3rd ed. (Oxford U. P., London, 1954), p. 181ff.

[23]A. Abragam and B. Bleaney, *Electron Paramagnetic Resonance of Transition Ions* (Oxford U. P., London, 1970).

[24]A. J. Freeman and R. E. Watson, in *Magnetism*, edited by G. T. Rado and H. Suhl (Academic, New York, 1965), Vol. IIA, p. 167ff.

[25]Z. J. Kiss, Phys. Rev. 127, 718 (1962).

[26]B. Bleaney, Proc. R. Soc. A 277, 289 (1964).

[27]R. G. Bessent and W. Hayes, Proc. R. Soc. A 284, 430 (1965).

[28]D. R. Huffman and M. H. Norwood, Phys. Rev. 117, 709 (1960).

[29]D. R. Franceschetti, Ph.D. thesis (Princeton University, 1973) (unpublished).

[30]The same considerations apply to Ref. 9, in which Eq. (5.18) should read

$$T^{ij}_{\text{Raman}} = \frac{9!\,\hbar^2}{2\pi^3\rho^2 v^{10}}\left(\frac{kT}{\hbar}\right)^9 V_R(i,j)\ ,$$

and in Eqs. (5.19), (5.25), and (5.26) the term $1/\Delta_t$ should be changed to $1/\Delta_t^2$. We thank Professor George Seidel for correspondence concerning this matter.

[31]E. S. Sabisky and C. H. Anderson, Phys. Rev. B 1, 2029 (1970).

[32]R. G. Barnes, R. L. Mössbauer, E. Kankeleit, and J. M. Pointdexter, Phys. Rev. 136, A175 (1964).

[33]H. A. Weakleim and Z. J. Kiss, Phys. Rev. 157, 277 (1967).

[34]H. R. Lewis and E. S. Sabisky, Phys. Rev. 130, 1370 (1963).

[35]E. Belorisky, Y. Ayant, D. Descamps, and Y. Merle d'Aubigné, J. Phys. 27, 313 (1966).

[36]D. Descamps and Y. Merle d'Aubigné, Phys. Lett. 8, 5 (1964).

[37]S. Bhagavantam, Proc. Indian Acad. Sci. A 41, 72 (1955).

[38]M. B. Walker, Can. J. Phys. 46, 1347 (1968).

[39]H. Callen and V. G. Baryakhtar, Phys. Rev. B 6, 1010 (1972).

[40]M. Tinkham, *Group Theory and Quantum Mechanics* (McGraw-Hill, New York, 1964), p. 40ff.

[41]M. Reed and B. Simon, *Methods of Mathematical Physics* (Academic, New York, 1972), Vol. I, p. 36ff.